Title

Elucidating the role of Vif-RNA and arms race interfaces in binding and promoting A3G ubiquitination

ISBN

9798270226268

Author

Dailey, Leandrew Allen

Publication Date

2025-12-17

Peer reviewed|Thesis/dissertation

Elucidating the role of Vif-RNA and arms race interfaces in binding and promoting A3G ubiquitination

by
Leandrew Allen Dailey

DISSERTATION
Submitted in partial satisfaction of the requirements for degree of
DOCTOR OF PHILOSOPHY

in

Chemistry and Chemical Biology

in the

GRADUATE DIVISION
of the
UNIVERSITY OF CALIFORNIA, SAN FRANCISCO

Approved:

DocuSigned by:
John Gross
C876331A93DC4B1...

John Gross
Chair

DocuSigned by:
Alan Frankel
DocuSigned by:
David Toczyski
402B6252FD6D45E...

Alan Frankel

David Toczyski

Committee Members

ACKNOWLEDGEMENTS

Words will never be enough to fully express my gratitude to the communities, my family, and friends who have kept me sane these last few years. I am constantly inspired by the people in my life, both those present and those who have passed away. As well as the deep history of the place I've been fortunate enough to call home since 2019. When HIV/AIDS was first discovered in the U.S. in June 1981, it would be more than four years before Ronald Regan publicly mentioned HIV/AIDS in September 1985. By the end of 1985, over 12,000 people had died from AIDS, and the number was growing rapidly. Regan would not begin implementing policy against HIV/AIDS until the end of his presidency in 1988. Stigma and fear of the sexual and gender non-normative materialized as queer contagion in the form of HIV-1.

Abandoned by the state, many queer and trans people took efforts against HIV/AIDS into their own hands to survive a virus rapidly killing them and their communities. I am inspired by individuals like the late Miss Major Griffin-Gracy (October 25, 1946 – October 13, 2025), who operated the first mobile needle exchange in San Francisco during the height of the AIDS crisis in the 1980s. Driving the van in places like the Tenderloin, Major organized an HIV prevention model that helped curb the spread of HIV as the U.S. government failed to address AIDS fully. This inaction was further challenged by direct action groups, such as Stop AIDS Now or Else.

Eighty activists shut down the Golden Gate Bridge on the morning of January 21st, 1989. Holding banners that read "AIDS = Genocide; Silence = Death; Fight Back." The goal of the action was to directly confront a world inactive against AIDS. Before I began to learn about HIV-1 on a molecular level, my perception of HIV/AIDS was shaped by similar histories and stigma. I moved to San Francisco in 2019 with a deep desire to learn more about HIV-1 in a city I knew very little about. I am grateful to this city, which I have called home over the last few years, and my friends and communities, with whom I have learned these specific histories of HIV/AIDS while I studied Vif in binding and ubiquitination assays.

I also want to express gratitude to my mentor, Dr. John Gross, who allowed me to learn about HIV on the molecular level and has always been supportive and encouraging. Thanks to my thesis committee members, whose guidance helped inform this work, Drs. Alan Frankel, Dave Toczyski, and Stephen Floor. Everyone in the Gross Lab has also been a great source of support over the last few years. Gabriel Braun was incredibly helpful in helping develop the Molecular Glue Assay described in Chapter 2. Thanks also to Trase Aguigam and Estelle Ronayne, who always offered help, feedback, questions, and engaging conversations.

I'd also like to thank Victor Lam, who was my rotation mentor during my first year, for teaching me how the Gross Lab performs ubiquitination assays. Xi, Yange, and Yen-Li were always willing to help and have been fun to learn from regarding Vif-APOBEC interactions, insect cell expression, and protein purification. Wooyoung Choi was invaluable with F-SEC experiments. All the invisible labor at UCSF. Thank you also to Dr. Hiroshi Matsuo, who provided help with expressing and purifying sA3G. Drs. Jon Lai and Elisabeth Nyakatura were my mentors at the PREP program I attended at the Albert Einstein College of Medicine, before I came to UCSF. Dr. Nyakatura was incredibly supportive during my graduate application process, and I honestly could not have gotten into UCSF without her help.

Drs. Les Sommerville and Steven Fenster were instrumental in my early development as a scientist and played a significant role in my decision to pursue a PhD during my time at Fort Lewis College in Durango, CO. Marjorie Beno, who was my middle school science teacher, sparked my interest in science when I was still a Rez kid on the Navajo Nation. My mother, who endlessly and unconditionally sacrificed to ensure the success of my siblings and me. The friends and family lost along the way who helped me create this life. To the friends and family who have held me and my emotions over these last few years. To the lives lost to HIV/AIDS and all forms of genocide. To my ancestors and the ancestors of the Ramaytush Ohlone people, who are the original inhabitants of this occupied land. Long live California NDNs.

Elucidating the role of Vif-RNA and arms race interfaces in binding and promoting A3G ubiquitination

Leandrew A. Dailey

ABSTRACT

Human APOBEC3G (A3G) is a potent cellular restriction factor against HIV-1. The viral protein Vif hijacks a Cullin5 RING (CRL5) E3 ubiquitin ligase to polyubiquitinate A3G for proteasomal degradation, neutralizing its antiviral potency. An ancient Molecular Arms race between lentiviruses and primate hosts modulates the Vif-A3G protein interface. Recently, we demonstrated in a cryo-EM structure that HIV-1 Vif also uses an RNA oligonucleotide as a molecular glue to bind A3G for polyubiquitination. Vif binds RNA and A3G in a manner that is compatible with polyubiquitination by coenzymes in the CRL5 complex. Vif utilizes RNA-binding to bind conserved residues in A3G, limiting its ability to escape antagonism. We demonstrate that RNA acts as a molecular glue, promoting the complex assembly of Vif and A3G. The role of RNA in promoting A3G ubiquitination is investigated using quantitative pulse-chase assays that monitor A3G mono-ubiquitination. The study of Vif-A3G binding, mediated by different interfaces including the molecular arms race and RNA, is coupled with quantitative ubiquitination assays in this work. A comprehensive understanding of this relationship can further reveal how viral adaptations manifest at the levels of binding and biochemistry.

TABLE OF CONTENTS

LIST OF FIGURES

Chapter 1: Introduction

Chapter 2: RNA is a Molecular Glue that promotes HIV-1 Vif binding to a solubility optimized human APOBEC3G variant

Chapter 3: APOBEC3G mono-ubiquitination catalyzed by Neddylated CRL5-Vif-CBFβ and ARIH2 is detected by fluorescent ubiquitin

Chapter 4: Future Directions

LIST OF ABBREVIATIONS

AIDS – Acquired Immunodeficiency Syndrome

A3F – apolipoprotein B mRNA editing enzyme, catalytic subunit 3F

A3G – apolipoprotein B mRNA editing enzyme, catalytic subunit 3G

ARIH2 – Ariadne RBR E3 Ubiquitin Protein Ligase 2

CBFβ – Core Binding Factor beta

CRL5 – Cullin-RING ubiquitin ligase 5

CD – Cytidine Deaminase

F-SEC – Fluorescence Size Exclusion Chromatography

HIV – Human Immunodeficiency Virus

MP – Mass Photometry

N8 – NEDD8

SIV – Simian Immunodeficiency Virus

sA3G – Soluble A3G

UB – Ubiquitin

UBE2L3 – Ubiquitin-conjugating enzyme E2 L3

VCBC – Vif-CBFβ-EloB-EloC

Chapter 1

INTRODUCTION

Millions of years of viral adaptation and zoonotic transmission events culminated in one of history's most significant pandemics, when Acquired Immunodeficiency Syndrome (AIDS) was first discovered in the early 1980s. Human Immunodeficiency Virus (HIV) was found to be the causative agent of AIDS in 1983.[1] HIV is a lentivirus belonging to the family of retroviruses, which infects several types of immune cells, primarily CD4+ T cells. As of 2025, it is estimated that up to 53.4 million people have died due to AIDS-related illnesses (UNAIDS).[2] Of the two major strains of HIV that infect humans, HIV-1 is the globally prevalent strain, while HIV-2 has been largely confined to countries in West Africa.

Both viruses originate from precursor lentiviruses that infect non-human primates known as Simian Immunodeficiency Viruses (SIVs). HIV-1 emerged from a cross-species transmission event of lentiviruses from Old-World Monkeys into hominid primates (**Fig. 1.1a**). More specifically, a strain of lentiviruses crossed over from Red Capped Mangabeys (SIVrcm) into Chimpanzees (SIVcpz).[3] Following the emergence of lentiviruses among hominid primates, these viruses became capable of infecting humans. On a molecular level, adaptation of the viral protein Vif played a significant role in enabling lentiviruses to overcome potent genetic barriers encoded by hominid primate hosts.

Vif comes from SIVrcm and its primary function is to overcome the antiviral host protein APOBEC3G (A3G).[4] Vif counteracts A3G by hijacking a Cullin5 RING (CRL5) E3 ubiquitin ligase serving as a cognate substrate receptor to bind and target A3G for proteasomal degradation.[5–8] Hominid primate A3G is a potent barrier to precursor lentiviruses from Old-World Monkeys, these viruses must equip a Vif capable of neutralizing host A3G to ensure their survival. There is an ancient Molecular Arms Race between Vif and A3G, meaning SIVrcm Vif adapted to overcome hominid primate A3G.[9,10] Over millions of years of primate evolution, primate A3G has undergone diversifying selection to escape antagonism by Vif, thereby allowing the host to

survive. In turn, the virus adapts to overcome A3G, regaining the ability to infect the host. These repeated bouts of host escape and viral adaptation are referred to as molecular arms races. The adaptation of SIVrcm to hominid primate A3G was a manifestation of this phenomenon and underlies the ancient origin of the AIDS pandemic.

A3G's antiviral activity comes from packaging into viral particles during an infection, where it can enzymatically alter C-to-U residues on the nascent ssDNA viral genome generated by reverse transcription.[11–13] A3G is a double-domain cytosine deaminase: the N-terminal domain is referred to as CD1, and the C-terminal domain is referred to as CD2.[14] The CD1 domain mediates RNA binding and is the primary domain that binds Vif.[11,12,15,16] The CD2 domain catalytically acts on the nascent single-stranded DNA (ssDNA) molecule of the viral genome, which is generated during reverse transcription.[13] Since the discovery of Vif-mediated proteasomal degradation of A3G, there has been significant interest in characterizing how these two proteins interact on a molecular level.

This has been difficult for various reasons – Vif is an intrinsically disordered protein that adopts a minimally folded confirmation with the transcription co-factor CBFβ.[17] Once folded, Vif can associate with the adapter proteins of the CRL5 E3 ubiquitin ligase, ElonginB and ElonginC, to form a substrate receptor complex known as **VCBC** (**V**if, **C**BFβ, Elo**B**, Elo**C**) (**Fig. 1.2a**). Biochemically, Vif is stably co-expressed and purified as VCBC. On the other hand, A3G oligomerizes with RNA, is poorly soluble, and prone to aggregation.[18] Prior to the development of any structures, the Vif-A3G interface was largely elucidated through genetic and viral infectivity assays, coupled with biochemical experiments.

Initial studies of Vif elucidated the interfaces critical for engaging other CRL5 ligase components, which are required for A3G degradation. A conserved ^{145}SLQ^{147} motif was shown to be crucial for engaging EloC.[19,20] Likewise, a novel zinc-binding HCCH motif, similar to canonical Cullin substrate receptor BC-box motifs, was shown to be essential for binding Cullin5.[21–23] The Vif-A3G interface was first uncovered through species-specificity experiments

with Vif, which demonstrated that residue D128 of human A3G determines the species specificity of HIV-1 Vif.[24–26] When mutated to K128, human A3G loses the ability to bind HIV-1 Vif but gains the ability to recognize several SIV Vif variants. Later studies demonstrated that additional residues at positions 129 and 130 of human A3G seemed to be crucial for also engaging Vif[16]. The region of Vif, $D^{14}RMR^{17}$, was believed to interact with D128 of human A3G, based on further species-specificity experiments.[27]

In a separate study comparing A3G and A3F recognition with various Vif mutations, $D^{14}RMR^{17}$ was found to be more crucial for A3F binding.[28] This study also revealed a hydrophobic patch of Vif, $Y^{40}RHHY^{44}$, critical for engaging A3G. An additional patch of residues, including K22, K26, and Y30, was later revealed to be important for binding A3G.[29,30] The residues spanning from 81 to 89 of Vif were found to be highly conserved among lentiviral Vif variants, and altering some of these residues was shown to affect binding to A3G.[31,32] Collectively, these early studies helped shape an understanding of the Vif-A3G interface, despite the absence of high-resolution structures.

In 2014, the first nearly full-length structure of Vif as the VCBC substrate receptor in complex with the N-terminal domain of Cullin-5 was reported.[33] This structure helped provide a structural understanding of how Vif hijacks the Cullin5 RING E3 ubiquitin ligase. Moreover, it enabled speculation about the interface that Vif might use to engage A3G. The second high-resolution structure of Vif came from a crystal structure of SIVrcm Vif in complex with human co-factors CBFβ, EloB, and EloC.[34] By comparing the structures of SIVrcm Vif with those of HIV-1 Vif, the researchers identified structural variations in the loop regions of Vif.

Careful mutagenesis experiments based on sequence comparisons of loop 5 in Vif, residues 81-84 of HIV-1 Vif, determined a single amino acid that determines species specificity towards hominid primate A3G variants. Y86 in SIVrcm Vif, when altered to a histidine or glutamine, like those observed at the corresponding residue in SIVcpz or HIV-1 Vif, respectively, gained the ability to bind and degrade human A3G. This became one of the first clues as to

what specific residues in HIV-1 Vif bind A3G. Without an A3G structure, it was difficult to identify which residues of Q83 of HIV-1 Vif interacted with.

Structural studies of A3G have been far more challenging due to its poor solubility and the inability to obtain homogeneous samples. Several variants of A3G have been generated, including mutations to CD1 to render A3G more soluble for structural studies.[35–37] The soluble variant of CD1 helped propose a binding mode for Vif on A3G. Likewise, other structures of A3G helped characterize A3G recognition for non-Vif substrates such as RNA and ssDNA. It would take more than 20 years after the initial discovery of the Vif-A3G interaction for high-resolution structures to become available.

In 2023, three cryo-EM structures of Vif bound to A3G were reported.[38–40] The Gross Lab generated the first structure using full-length and wild-type versions of both proteins (**Fig. 1.1b**). Interactions between Vif and A3G were validated across all three structures. Collectively, these structures provided a visualization of the Vif-A3G interface for the first time, validating the role of several residues listed above (**Fig. 1.1c**). R15 and Q83 of Vif were shown to engage D128 and D130 of human A3G, respectively. These residues form a protein-protein interface referred to as the Molecular Arms Race interface due to residues undergoing viral adaptation or diversifying selection. The presence of ssRNA mediating several other interactions between Vif and A3G was quite surprising. We believe that RNA serves as a molecular glue, promoting a high-affinity interaction between Vif and A3G.

More specifically, four nucleotides were observed making several contacts with Vif and A3G residues. While it was initially a shock, this should not be surprising given A3G's extensive ability to bind RNA. Furthermore, Vif binds A3G and RNA in a manner that is compatible with ubiquitination by co-enzymes recruited by the full CRL5-Vif-CBFβ ubiquitin ligase (**Fig. 1.2b**). Studying the biochemistry and enzymology of Vif-mediated ubiquitination of A3G has been of interest due to therapeutic potential in restoring A3G antiviral activity against HIV-1. Prior biochemistry experiments have primarily consisted of co-immunoprecipitation assays, qualitative

western blots, and other *in vivo* techniques. Furthermore, RNA has rarely been used as a variable in prior biochemistry experiments examining the assembly of the Vif-A3G complex and ubiquitination.

In chapter 2, we present a functional Molecular Glue Assay that can monitor Vif-A3G assembly as a function of RNA oligonucleotide. This interaction can be abolished by mutating Vif residues implicated in binding the RNA molecular glue that bridges the Vif-A3G interaction. I was also interested in determining whether we could observe this RNA-mediated effect on A3G ubiquitination. In Chapter 3, I present a pulse-chase ubiquitination assay to measure A3G mono-ubiquitination catalyzed by the CRL5-Vif-CBFβ ubiquitin ligase quantitatively. Part of this work aims to understand better the relationship between the Vif-A3G-RNA interface, the Molecular Arms Race interface, and A3G ubiquitination. Before the discovery of RNA in the Vif-A3G interface, a simple model of Vif-A3G binding was considered to ensure adequate ubiquitination and neutralization of A3G; however, this model may not be correct.

The binding mode of Vif and A3G is investigated in this work to determine whether binding is a sufficient process for A3G ubiquitination and its subsequent neutralization. I hypothesize that binding is inadequate and Vif must bind A3G in a manner that properly orients it for ubiquitination to ensure adequate neutralization. Overall, this work is at the forefront of carefully examining the relationship between host-virus molecular arms races, RNA binding, and quantitative ubiquitination enzymology.

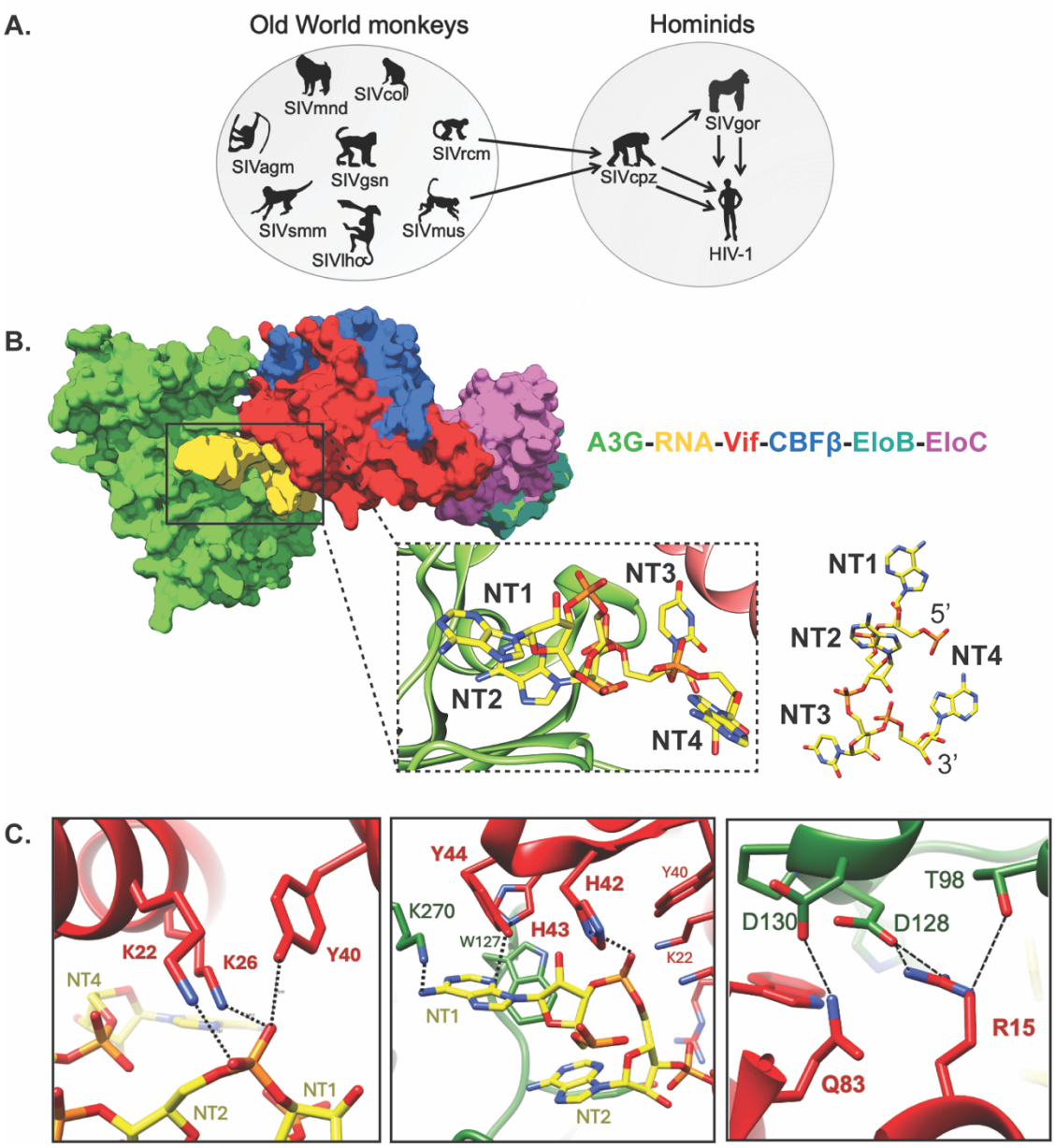

Figure 1.1: Overview of Vif-A3G binding A) Schematic of cross-species transmission of lentiviruses from Old World monkeys into Hominid primates and the origin of HIV-1. **B)** Cyro-EM structure of wild-type A3G bound to the HIV-1 Vif substrate receptor complex VCBC **(**Vif, CBFβ, EloB, EloC) and RNA. The four-nucleotide core is shown. **C)** Close-up of different interfaces that occur between HIV-1 Vif and A3G.

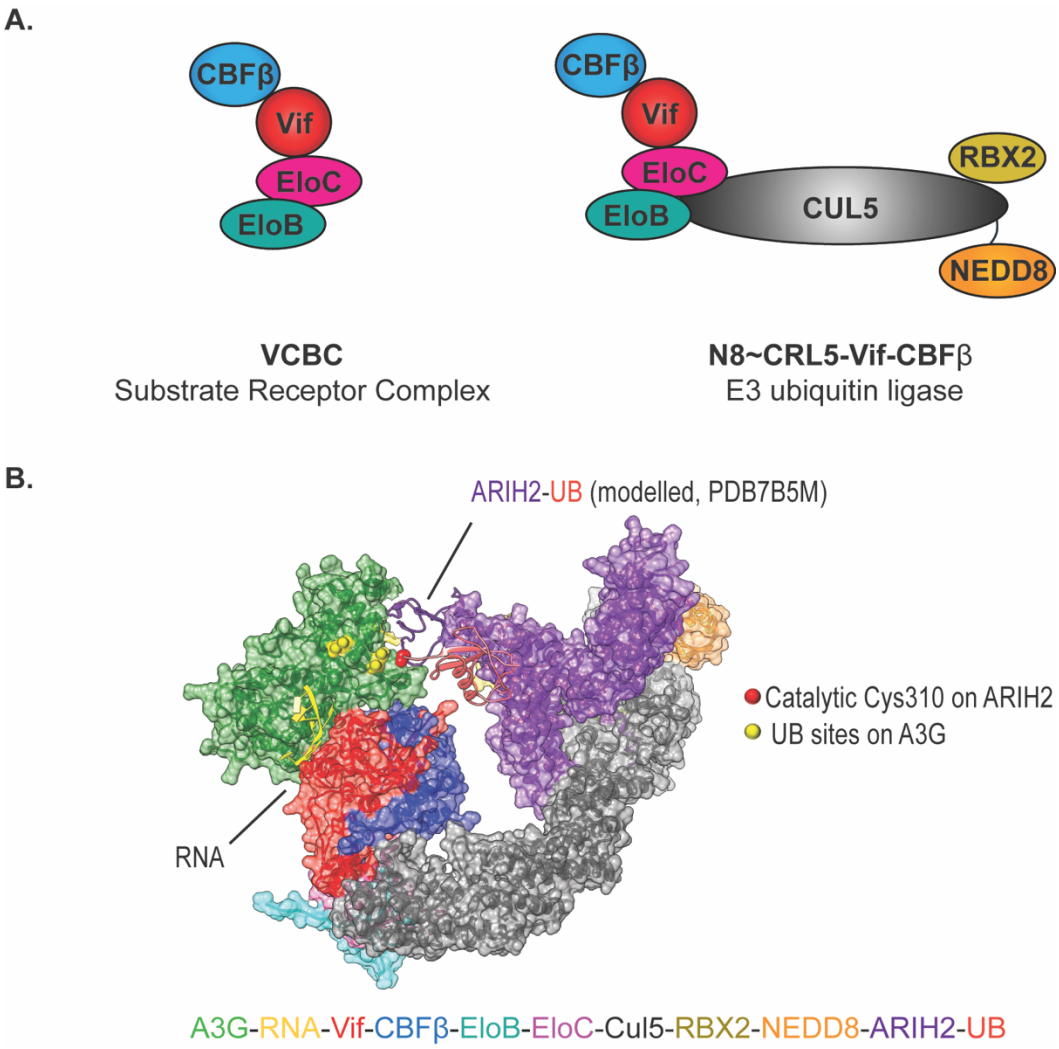

Figure 1.2: VCBC substrate receptor complex versus full E3 ubiquitin ligase A) Vif in complex with other protein components to form the substrate receptor complex (left) compared to all components of the E3 ubiquitin ligase (right). **B)** Homology model of Vif bound to RNA, A3G, the other protein components of the E3 ubiquitin ligase, and ARIH2 thioester bound with ubiquitin.

REFERENCES

1. Barré-Sinoussi, F. *et al.* Isolation of a T-Lymphotropic Retrovirus from a Patient at Risk for Acquired Immune Deficiency Syndrome (AIDS). *Science* **220**, 868–871 (1983).
2. Global HIV & AIDS statistics — Fact sheet | UNAIDS.
3. Bailes, E. *et al.* Hybrid Origin of SIV in Chimpanzees. *Science* **300**, 1713–1713 (2003).
4. Etienne, L., Hahn, B. H., Sharp, P. M., Matsen, F. A. & Emerman, M. Gene loss and adaptation to hominids underlie the ancient origin of HIV-1. *Cell Host Microbe* **14**, 85–92 (2013).
5. Yu, X. *et al.* Induction of APOBEC3G Ubiquitination and Degradation by an HIV-1 Vif-Cul5-SCF Complex. *Science* **302**, 1056–1060 (2003).
6. Conticello, S. G., Harris, R. S. & Neuberger, M. S. The Vif Protein of HIV Triggers Degradation of the Human Antiretroviral DNA Deaminase APOBEC3G. *Curr. Biol.* **13**, 2009–2013 (2003).
7. Liu, B., Yu, † Xianghui, Luo, † Kun, Yu, Y. & Yu, X.-F. Influence of Primate Lentiviral Vif and Proteasome Inhibitors on Human Immunodeficiency Virus Type 1 Virion Packaging of APOBEC3G. *J. Virol.* **78**, 2072–2081 (2004).
8. Mehle, A. *et al.* Vif Overcomes the Innate Antiviral Activity of APOBEC3G by Promoting Its Degradation in the Ubiquitin-Proteasome Pathway. *J. Biol. Chem.* **279**, 7792–7798 (2004).
9. Daugherty, M. D. & Malik, H. S. Rules of engagement: Molecular insights from host-virus arms races. *Annu. Rev. Genet.* **46**, 677–700 (2012).
10. Compton, A. A., Malik, H. S. & Emerman, M. Host gene evolution traces the evolutionary history of ancient primate lentiviruses. *Philos. Trans. R. Soc. B Biol. Sci.* **368**, 20120496 (2013).
11. Zennou, V., Perez-Caballero, D., Göttlinger, H. & Bieniasz, P. D. APOBEC3G Incorporation into Human Immunodeficiency Virus Type 1 Particles. *J. Virol.* **78**, 12058–12061 (2004).

12. Svarovskaia, E. S. *et al.* Human Apolipoprotein B mRNA-editing Enzyme-catalytic Polypeptide-like 3G (APOBEC3G) Is Incorporated into HIV-1 Virions through Interactions with Viral and Nonviral RNAs. *J. Biol. Chem.* **279**, 35822–35828 (2004).
13. Harris, R. S. *et al.* DNA Deamination Mediates Innate Immunity to Retroviral Infection. *Cell* **113**, 803–809 (2003).
14. Navarro, F. *et al.* Complementary function of the two catalytic domains of APOBEC3G. *Virology* **333**, 374–386 (2005).
15. Khan, M. A. *et al.* Analysis of the contribution of cellular and viral RNA to the packaging of APOBEC3G into HIV-1 virions. *Retrovirology* **4**, 48 (2007).
16. Huthoff, H. & Malim, M. H. Identification of Amino Acid Residues in APOBEC3G Required for Regulation by Human Immunodeficiency Virus Type 1 Vif and Virion Encapsidation. *J. Virol.* **81**, 3807–3815 (2007).
17. Jäger, S. *et al.* Vif hijacks CBF-β to degrade APOBEC3G and promote HIV-1 infection. *Nature* **481**, 371–375 (2012).
18. Huthoff, H., Autore, F., Gallois-Montbrun, S., Fraternali, F. & Malim, M. H. RNA-Dependent Oligomerization of APOBEC3G Is Required for Restriction of HIV-1. *PLOS Pathog.* **5**, e1000330–e1000330 (2009).
19. Marin, M., Rose, K. M., Kozak, S. L. & Kabat, D. HIV-1 Vif protein binds the editing enzyme APOBEC3G and induces its degradation. *Nat. Med.* **9**, 1398–1403 (2003).
20. Yu, Y., Xiao, Z., Ehrlich, E. S., Yu, X. & Yu, X. F. Selective assembly of HIV-1 Vif-Cul5-ElonginB-ElonginC E3 ubiquitin ligase complex through a novel SOCS box and upstream cysteines. *Genes Dev.* **18**, 2867–2872 (2004).
21. Paul, I., Cui, J. & Maynard, E. L. Zinc binding to the HCCH motif of HIV-1 virion infectivity factor induces a conformational change that mediates protein–protein interactions. *Proc. Natl. Acad. Sci.* **103**, 18475–18480 (2006).

22. Xiao, Z. *et al.* Assembly of HIV-1 Vif-Cul5 E3 ubiquitin ligase through a novel zinc-binding domain-stabilized hydrophobic interface in Vif. *Virology* **349**, 290–299 (2006).
23. Giri, K., Scott, R. A. & Maynard, E. L. Molecular Structure and Biochemical Properties of the HCCH−Zn2+ Site in HIV-1 Vif. *Biochemistry* **48**, 7969–7978 (2009).
24. Mariani, R. *et al.* Species-Specific Exclusion of APOBEC3G from HIV-1 Virions by Vif. *Cell* **114**, 21–31 (2003).
25. Schröfelbauer, B., Chen, D. & Landau, N. R. A single amino acid of APOBEC3G controls its species-specific interaction with virion infectivity factor (Vif). *Proc. Natl. Acad. Sci.* **101**, 3927–3932 (2004).
26. Xu, H. *et al.* A single amino acid substitution in human APOBEC3G antiretroviral enzyme confers resistance to HIV-1 virion infectivity factor-induced depletion. *Proc. Natl. Acad. Sci.* **101**, 5652–5657 (2004).
27. Schröfelbauer, B., Senger, T., Manning, G. & Landau, N. R. Mutational Alteration of Human Immunodeficiency Virus Type 1 Vif Allows for Functional Interaction with Nonhuman Primate APOBEC3G. *J. Virol.* **80**, 5984–5991 (2006).
28. Russell, R. A. & Pathak, V. K. Identification of Two Distinct Human Immunodeficiency Virus Type 1 Vif Determinants Critical for Interactions with Human APOBEC3G and APOBEC3F. *J. Virol.* **81**, 8201–8210 (2007).
29. Chen, G., He, Z., Wang, T., Xu, R. & Yu, X.-F. A Patch of Positively Charged Amino Acids Surrounding the Human Immunodeficiency Virus Type 1 Vif SLVx4Yx9Y Motif Influences Its Interaction with APOBEC3G. *J. Virol.* **83**, 8674–8682 (2009).
30. Dang, Y., Wang, X., Zhou, T., York, I. A. & Zheng, Y.-H. Identification of a Novel WxSLVK Motif in the N Terminus of Human Immunodeficiency Virus and Simian Immunodeficiency Virus Vif That Is Critical for APOBEC3G and APOBEC3F Neutralization. *J. Virol.* **83**, 8544–8552 (2009).

31. Dang, Y., Davis, R. W., York, I. A. & Zheng, Y.-H. Identification of 81LGxGxxIxW89 and 171EDRW174 Domains from Human Immunodeficiency Virus Type 1 Vif That Regulate APOBEC3G and APOBEC3F Neutralizing Activity. *J. Virol.* **84**, 5741–5750 (2010).
32. Dang, Y., Wang, X., York, I. A. & Zheng, Y.-H. Identification of a Critical T(Q/D/E)x5ADx2(I/L) Motif from Primate Lentivirus Vif Proteins That Regulate APOBEC3G and APOBEC3F Neutralizing Activity. *J. Virol.* **84**, 8561–8570 (2010).
33. Guo, Y. *et al.* Structural basis for hijacking CBF-β and CUL5 E3 ligase complex by HIV-1 Vif. *Nature* **505**, 229–233 (2014).
34. Binning, J. M., Chesarino, N. M., Emerman, M. & Gross, J. D. Structural Basis for a Species-Specific Determinant of an SIV Vif Protein toward Hominid APOBEC3G Antagonism. *Cell Host Microbe* **26**, 739-747.e4 (2019).
35. Kouno, T. *et al.* Structure of the Vif-binding domain of the antiviral enzyme APOBEC3G. *Nat. Struct. Mol. Biol.* **22**, 485–491 (2015).
36. Maiti, A. *et al.* Crystal Structure of a Soluble APOBEC3G Variant Suggests ssDNA to Bind in a Channel that Extends between the Two Domains. *J. Mol. Biol.* **432**, 6042–6060 (2020).
37. Yang, H. *et al.* Understanding the structural basis of HIV-1 restriction by the full length double-domain APOBEC3G. *Nat. Commun.* **11**, 632 (2020).
38. Li, Y.-L. *et al.* The structural basis for HIV-1 Vif antagonism of human APOBEC3G. *Nature* **615**, 728–733 (2023).
39. Kouno, T. *et al.* Structural insights into RNA bridging between HIV-1 Vif and antiviral factor APOBEC3G. *Nat. Commun.* **14**, 4037 (2023).
40. Ito, F. *et al.* Structural basis for HIV-1 antagonism of host APOBEC3G via Cullin E3 ligase. *Sci. Adv.* **9**, eade3168 (2023).

CHAPTER 2

RNA is a Molecular Glue that promotes HIV-1 Vif binding to a solubility optimized human APOBEC3G variant

ABSTRACT

Previous structural studies have demonstrated RNA is a cofactor for binding between HIV-1 Vif and human APOBEC3G (A3G). The presence of ssRNA has been observed deeply sandwiched between Vif and A3G in several cryo EM structures. RNA is believed to serve as a molecular glue by increasing the buried surface area between Vif and A3G by creating a distinct Vif-RNA-A3G interface. Several Vif residues mediate interactions with both RNA and A3G in this interface, including H43 and Y44. To test the hypothesis that RNA acts as a molecular glue, we developed a functional assay using Mass Photometry to demonstrate RNA-mediated formation of Vif bound to a solubility-enhanced human A3G variant (sA3G). To validate this binding assay, we used a previously described double-alanine negative control of Vif, in which both H43 and Y44 of Vif have been altered to alanine residues, which reduces HIV-1 Vif binding to human A3G. We also attempted to develop a similar molecular glue assay with wild-type human A3G, but demonstrate that the presence of co-purified RNA with wild-type A3G is difficult to remove entirely.

INTRODUCTION

After the discovery of HIV-1 as a causative agent of AIDS, much work went into characterizing the genes encoded by the virus.[1,2] HIV-1 Vif was initially discovered in 1986 in an overlapping reading frame on the 3' terminus of the *pol* gene.[3] In 1987, it was demonstrated that Vif was required for viral infection, despite its initial classification as an accessory protein.[4,5] Early functional studies of Vif using virions lacking a functional *vif* gene demonstrated that it was capable of infecting permissive cells but unable to infect non-permissive cells.[6] By the end of the 1990s, speculation arose that an unknown host restriction factor was expressed in non-permissive cells, which could potently inhibit *vif*-deficient virions.

The unknown restriction factor was discovered in 2002, initially named CEM15, it was later renamed to APOBEC3G based on sequence homology to APOBEC1, a previously identified cytidine deaminase.[7,8] Shortly after, A3G was shown to inhibit HIV-1 by packaging into viral particles and hypermutating the viral genome.[9–11] A3G is packaged into viral particles based on RNA-dependent interactions mediated by residues in its N-terminal CD1 domain.[12] The CD1 domain also dictates A3G oligomerization through its RNA-binding properties. A3G has been shown to be associated with a wide variety of RNA molecules, often forming high-molecular-weight ribonucleoprotein complexes in cells.

RNA binding by A3G appears to be partly regulated by A3G preferentially binding to G-rich and A-rich sequences, such as those found in the HIV-1 RNA genome.[13] Additionally, newly synthesized, lower molecular weight mass A3G oligomers are preferentially packaged into viral particles.[14] Before the availability of high-resolution structures of Vif and A3G, Vif was assumed to bind A3G solely through protein-protein interactions. Interfaces like the Molecular Arms Race interface were characterized with little consideration for the possibility that RNA might serve as a cofactor in bridging these two proteins together. However, as we observed in our structure, RNA is a molecular glue that increases the buried surface area between Vif and A3G, promoting a high-affinity interaction.[15]

In our cryo-EM structures, we observed two molecules of both Vif and A3G dimerized on a single ssRNA molecule in at least two distinct conformations (**Fig. S2.1**). One perplexing detail from these conformations is that, despite extensive research detailing A3G's self-association, Vif binds monomeric A3G in our structure. We hypothesize that Vif binds A3G early on in its synthesis before it can self-associate. However, this poses an issue for carefully reconstituting Vif-A3G for use in *in vitro* biochemistry experiments.

The goal of the work outlined in this chapter is to determine whether we can reconstitute Vif-A3G assembly as a function of RNA oligonucleotide. This work is essential to ensure biochemistry studies with Vif:RNA:A3G complexes accurately reflect what is observed structurally. Our functional Molecular Glue assay utilizes Mass Photometry to monitor the RNA-mediated assembly of HIV-1 Vif and a solubility-enhanced human A3G variant (sA3G) (**Fig. S2.3**). I also attempted to generate a Molecular Glue assay with wild-type A3G using Fluorescence Size Exclusion Chromatography (F-SEC). However, these attempts were unsuccessful due to our inability to fully remove co-purified RNA from wild-type A3G.

RESULTS

sA3G binds HIV-1 Vif in an RNA-dependent manner

Previous work has demonstrated successful RNA-mediated reconstitution of a sA3G-Vif-CBFβ complex using a 20-nucleotide single-stranded RNA oligomer referred to as RNA20.[16] Notably, this study employs an optimized Vif-CBFβ construct, rather than the ternary Vif-CBFβ-EloB-EloC (VCBC) substrate receptor complex, and utilizes Size Exclusion Chromatography to monitor the formation of sA3G-Vif-CBFβ complexes. We were interested in determining whether we could reconstitute this phenomenon using Mass Photometry (MP). When RNA20 is added to samples containing HIV-1 VCBC and sA3G, we expect an overall shift in the molecular weight and relative abundance of the sample.

MP is a biophysical technique that utilizes Rayleigh scattering to measure the molar mass of macromolecules and can quantify the relative number of unlabeled proteins in solution.[17] We used MP to measure the individual masses of HIV-1 VCBC and sA3G and compared them to a mixture of VCBC and sA3G with or without RNA20 added (**Fig. 2.1**). VCBC has an approximate molecular weight of ~70 kDa, sA3G has an expected molecular weight of ~44 kDa, and a complex of both components has an expected molecular weight of ~104 kDa. When individual components were measured with MP, the relative abundance of VCBC and sA3G correlated with their approximate molecular masses (**Fig. 2.1 red and blue**).

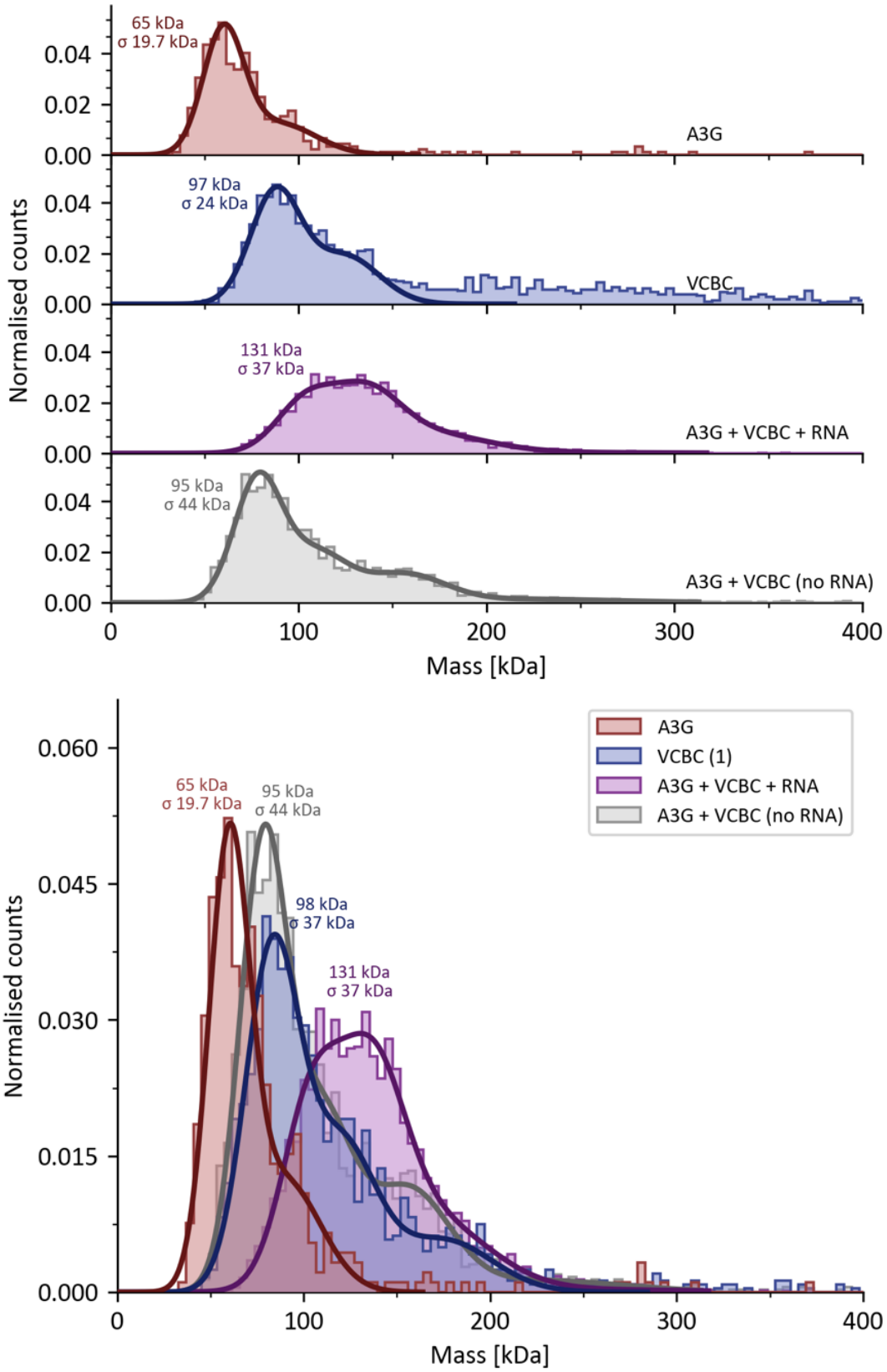

Figure 2.1: sA3G-VCBC assembly is formed when RNA20 is added. (continued next page)

Top) faceted mass histograms of sA3G (red), HIV-1 VCBC (blue), a mixture of sA3G and VCBC with RNA20 (purple), and a mixture of sA3G and VCBC with no RNA20 present (grey). Protein mass in kDa is represented on the x-axis, and the normalized counts of particles are shown on the y-axis. Counts were normalized across all counts measured in a sample **Bottom)** Overlaid mass histograms.

When RNA20 is added to a mixture of sA3G and VCBC (**Fig. 2.1, purple**), we observed an increase in the relative abundance of higher molecular weight complexes, which indicates the formation of a sA3G:VCBC complex. In contrast, when no RNA20 is added to the mixture, there is no shift in the relative abundance of proteins towards a higher molecular weight protein complex (**Fig. 2.1, grey**). The mass histogram of the sA3G:VCBC mixture with no RNA20 present is nearly identical to the mass histograms of the individual sub-components, indicating that a complex between both components was not formed. Furthermore, this demonstrates our ability to reconstitute an sA3G:VCBC complex in an RNA-mediated manner, as previously reported.

Next, we wanted to determine whether we could abolish the RNA-mediated interaction between Vif and sA3G using VCBC containing Vif with a double alanine mutation at positions H43 and Y44 in Vif. In our structure of wild-type Vif bound to human A3G, both H43 and Y44 of Vif are involved in the Vif-RNA-A3G interface (**Fig. 1.1c**). Both H43 and Y44 of Vif uniquely bind both RNA and A3G. The H43A/Y44A mutation in Vif has been shown to negatively impact binding to A3G in previous studies in cells.[18–20] We decided to test if this mutation can serve as a negative control in our Mass Photometry Molecular Glue Assay (**Fig. 2.2**). Since H43 and Y44 of Vif simultaneously bind A3G and RNA, we expect VCBC containing a Vif with this double alanine mutation will be unable to form a complex with sA3G and RNA20.

As expected, when VCBC containing Vif with the H43A/Y44A mutation was combined with sA3G and RNA20, the relative abundance of protein did not shift towards a higher molecular weight, indicating the complex was not formed (**Fig. 2.2, maroon**). In fact, the relative abundance of protein in this sample reflects the mass histograms of the individual sub-

components: sA3G (**Fig. 2.2, teal**) and H43A/Y44A VCBC (**Fig. 2.2, orange**). This contrasts with the wild-type VCBC, which demonstrates an increase in the relative abundance of a higher molecular weight protein, indicating the formation of a sA3G:VCBC complex (**Fig. 2.2, purple**). Overall, these experiments demonstrate RNA-mediated formation of Vif and sA3G, which can be abolished with a previously described Vif mutation that abrogates A3G antagonism in cells.

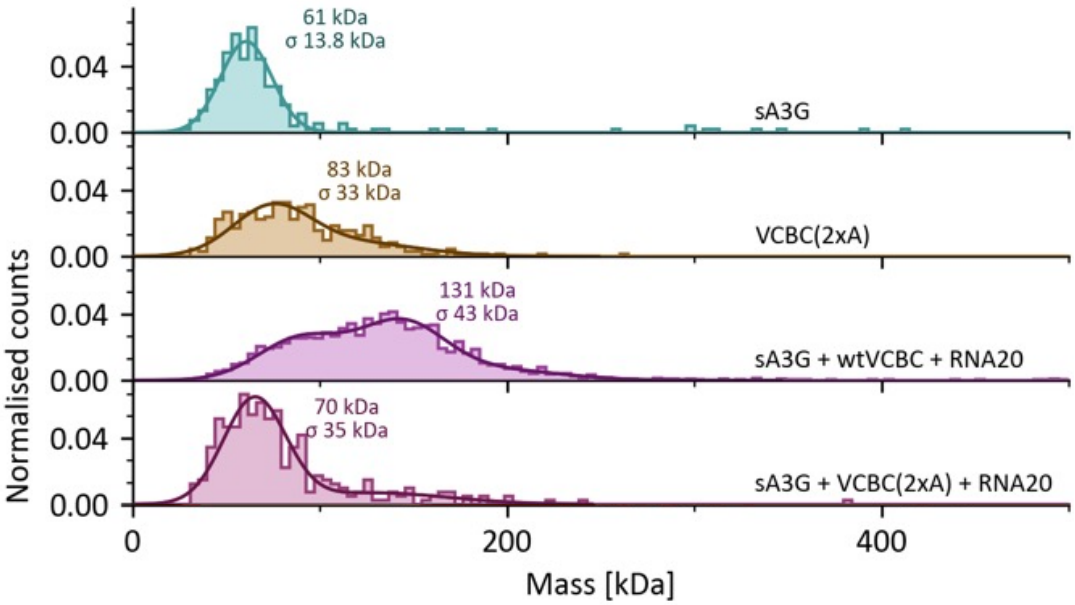

Figure 2.2: sA3G-VCBC assembly disrupted with Vif double-alanine mutation. Mass Histograms of sA3G (teal), H43A/Y44A VCBC (orange), and comparing assembly of sA3G:VCBC with RNA20 using wild type VCBC (purple) and H43A/Y44A VCBC (maroon). Protein mass in kDa is represented on the x-axis, and the normalized counts of particles are shown on the y-axis. Counts were normalized to.

Monomeric wild-type A3G is difficult to isolate due to copurified RNA

Our lab is one of the few to use wild-type A3G in *in vitro* biochemistry experiments. Wild-type A3G is stably purified from Sf9 insect cells as a dimer with co-purified RNA.[21] As previously stated, Vif binds monomeric A3G in our cryo EM structures. Using fluorescently labeled wild-type A3G, I aimed to determine if we could generate RNA-free monomeric A3G samples for use in RNA add-back experiments by treating wild-type A3G with RNase A/T1. We used F-SEC to selectively monitor fluorescent wild-type A3G that had been treated with RNase A/T1. In a

simple experiment, we treated fluorescent wild-type A3G with RNase A/T1 with increasing digestion times (**Fig. 2.3**). Hypothetically, as wild-type A3G is treated with RNase A/T1 for longer, we should expect conversion of the sample from a dimer to a monomer.

As expected, when wild-type A3G is treated with RNase A/T1, we observe a general decrease in the presence of dimeric A3G and an increase in the presence of monomeric A3G. However, even when wild-type A3G is treated with RNase A/T1 for up to 320 minutes (**Fig. 2.3, teal**), we do not observe complete conversion of dimeric A3G to monomeric A3G, indicating that copurified RNA is still present in the samples. Likewise, when the conditions of RNase A/T1 digestion are controlled at 240 minutes, the levels at which dimeric A3G is converted to monomeric A3G are not repeated between experiments (**Fig. S2.2**).

Wild-type A3G is purified from lysed Sf9 insect cells that are extensively treated with RNase A. Wild-type A3G is purified as a homogenous dimeric sample in the final sizing step of the overall protein purification. Theoretically, the RNA oligomer that co-purifies with wild-type A3G should also be homogenous, although the sequence and length of the co-purified RNA are not known. RNase A/T1 cleaves after pyrimidines and guanosines, respectively. It is possible that the RNA that co-purifies with wild-type A3G is not as homogeneous as we might expect, which could explain the variability in levels of monomeric A3G between digestions. Likewise, the co-purified RNA oligomer could be deeply wedged between copies of A3G, which might explain our inability to fully convert the A3G dimer to a monomer. Currently, we are unable to isolate an RNA-free, monomeric, wild-type A3G sample for use in RNA add-back experiments.

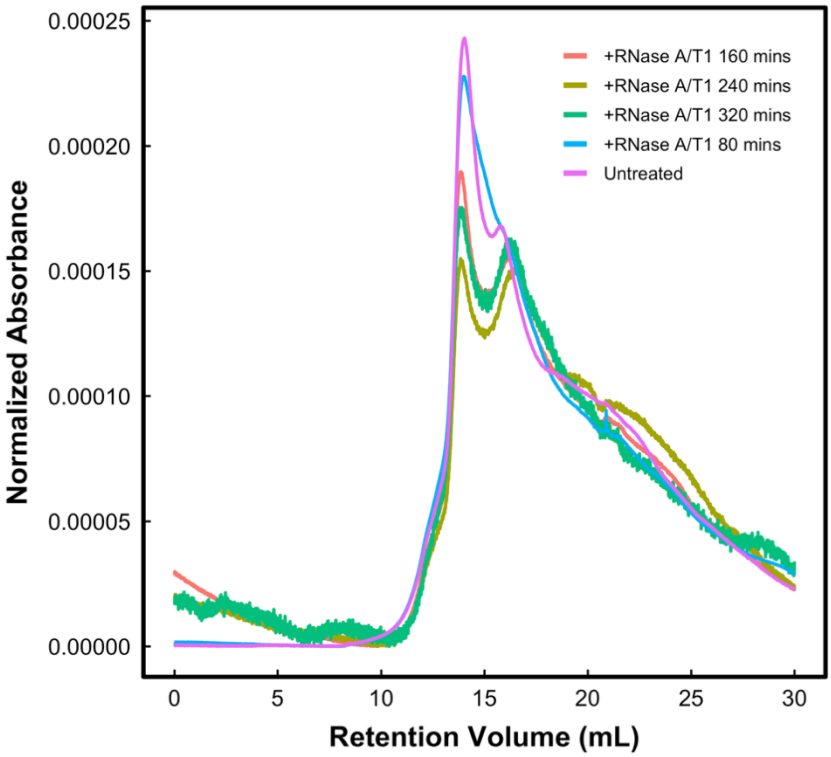

Figure 2.3: Monitoring wild-type A3G digested with RNase A/T1. Wild-type A3G was digested with RNase A/T1 at various incubation times, and reaction products were separated on a Superdex 200 column. Overlaid size exclusion chromatograms collected using an excitation wavelength of 488 nm and an emission wavelength of 508 nm. Each chromatogram was first normalized by baseline subtraction, so that the baseline starts at 0, and then normalized by area, ensuring that the sum of the total area under each curve equals 1. Dimeric A3G has an elution volume of ~14.5 mL.

DISCUSSION

RNA has previously been shown to be a cofactor for HIV-1 Vif and human A3G binding, leading to the hypothesis that RNA is a molecular glue that promotes a high-affinity interaction between the two proteins. We were interested in testing the hypothesis that RNA is a molecular glue that promotes Vif-A3G binding. Using a solubility-optimized human A3G variant (sA3G), we were able to demonstrate that HIV-1 Vif binds sA3G in an RNA-dependent manner using the RNA20 oligonucleotide (**Fig. S2.1**). By mutating two Vif residues that interact with both RNA and A3G at position H43 and Y44, binding between Vif and sA3G is disrupted when the two residues are altered to alanine (**Fig. 2.2**). We also wanted to determine whether we could test this hypothesis with wild-type A3G.

To test the role of RNA as a molecular glue with wild-type A3G, first requires generating a monomeric, RNA-free, wild-type A3G sample to use in RNA add-back experiments. To achieve this, we aimed to determine whether extensive RNase treatment with wild-type A3G was sufficient to convert dimeric wild-type A3G into monomeric A3G. We were unable to fully generate monomeric A3G, even with extensive RNase A/T1 treatment (**Fig. 2.3**), suggesting that the co-purified RNA is tightly bound and protected. Similarly, the conversion of dimeric A3G to monomeric A3G is non-reproducible, implying that the co-purified RNA may not be a homogeneous sample. Currently, this hinders our ability to test the RNA-mediated effect of Vif-A3G binding with wild-type A3G. However, we are pleased to report a functional assay using sA3G instead of wild-type A3G.

METHODS

Insect cell lines

Sf9 insect cells were obtained from ATCC and maintained in a 1X Sf-900 III SFM medium (Life Technologies Corporation #12658027) supplemented with heat-inactivated fetal bovine serum (Corning #35-011-CV) and 1% penicillin-streptomycin (Invitrogen 15140122). Cells were cultured at 27 °C and maintained in the dark for under two months before being returned to a lower-passage frozen stock.

Plasmids

A gene block containing the full-length, *E. coli* codon-optimized sequence of sA3G (Twist Biosciences, Inc.) was used as a template to generate PCR fragments with 5' and 3' overhangs for cloning into the pGEX-6P-1 vector.[16] The pGEX-6P-1 vector was PCR amplified to contain 5' and 3' overhangs with the full-length sequence of sA3G. PCR products were separated on a 1% agarose gel and then extracted from the gel using the QIAquick PCR Purification Kit (Qiagen #28106). pGEX-6P-1-sA3G was cloned by Gibson assembly using the gel-purified amplicons with an NEB HiFi DNA assembly kit (NEB #E2621).

Hxb2 Vif with a 6x-His tag and CBFβ were cloned onto a pET-Duet vector. Elongin B and Elongin C were cloned onto a pCDF plasmid as previously described. The pET-Duet vector was used as a template to generate the H43A/Y44A Vif mutation using site-directed mutagenesis. A KCK-tag was appended to the C-terminus of wild-type A3G, followed by a myc-tag, a TEV cleavage site, and GFP with a Strep-tagII, and cloned into a pFASTBAC vector. This pFASTBAC vector was used to generate baculoviruses for Sf9 insect cells.

Protein Expression and Purification

GST-sA3G was transformed into BL21 (DE3) cells (NEB #C2527H). The cells were grown at 37° C in LB media to an OD of 0.4-0.5, induced with 0.2 mM IPTG, and grown at 16 °C overnight. Cells were pelleted at 4000 rpm for 20 minutes at 4° C. Pelleted cells were resuspended and sonicated in sA3G Lysis Buffer (50 mM sodium phosphate, pH 7.3, 200 mM

NaCl, 50 μM $ZnCl_2$, 0.5% Triton X, 1 mM DTT) with Pierce™ Universal Nuclease for Cell Lysis (ThermoFisher #88702). The lysate was clarified by centrifugation at 20,000 rpm for 30 minutes at 4 °C. The clarified lysate was applied to Glutathione Sepharose™ 4B resin (Cytiva #17-0756-01) to immobilize GST-sA3G. Nucleases were removed with several high-salt washes using a buffer like sA3G Lysis Buffer, with the NaCl concentration decreasing from 1.5 M to 0.2 M. The immobilized protein was washed several times with Enzyme Cut Buffer (50 mM sodium phosphate, pH 7.3, 100 mM NaCl, 0.002% Tween 20, 1 mM EDTA). sA3G was liberated from Glutathione Sepharose™ 4B resin by incubating with PreScission Protease (GenScript Z02799-250) at 4° C overnight while rotating. After overnight incubation, the flowthrough with cleaved sA3G was collected, concentrated, and purified using Size Exclusion Chromatography with a Superdex SD200 column in sA3G Sizing Buffer (25 mM Tris-HCl, pH 8.0, 150 mM NaCl, 0.5 mM TCEP). Fractions corresponding to sA3G were pooled and concentrated.

Wild-type and mutant VCBC complexes were expressed and purified as previously described.[22] Briefly, plasmids containing Vif-CBFβ and EloB-EloC were co-transformed into BL21 cells (DE3). The cells were grown at 37° C in LB media to an optical density of 0.6-0.8 and induced with 0.5 mM IPTG overnight at 18° C. Cells were pelleted at 4000 rpm for 20 minutes at 4° C. VCBC was purified from cells resuspended and lysed via sonication in the following lysis buffer (25 mM Tris-HCl pH 8, 500 mM NaCl, 40 mM imidazole). Following centrifugation, the clarified lysate was loaded onto a nickel column (Cytiva #17524802) and washed with Nickel wash buffer (25 mM Tris-HCl, pH 8, 150 mM NaCl, 10 mM imidazole. VCBC was eluted from a nickel column on an FPLC using a gradient elution with two wash buffers varying in imidazole concentrations from 10 mM to 1 M imidazole. Eluted fractions corresponding to VCBC were pooled and collected. Imidazole was desalted by loading pooled fractions onto a Heparin column and washing with Heparin Wash Buffer (25 mM Tris-HCl, pH 8, 150 mM NaCl, 2 mM DTT). VCBC was eluted from the Heparin column using an FPLC with a gradient elution of high-salt Heparin wash buffer (25 mM Tris-HCl, pH 8, 1 M NaCl, 2 mM DTT). Fractions

corresponding to eluted VCBC were pooled, concentrated, and purified on an FPLC using size exclusion chromatography using a Superdex SD200 column with a sizing buffer (20 mM HEPES, pH 8, 300 mM NaCl, 10% Glycerol, and 1 mM DTT).

Wild-type A3G-KCK fused to GFP was expressed in Sf9 insect cells by infecting 1 L of cells with recombinant baculoviruses and incubating infected cells at 27° C in 1X Sf-900 III SFM media at 120 rpm. Cells were harvested 48 hours post-infection by centrifugation at 4000 rpm for 20 minutes at 4°C. Sf9 cells were resuspended in lysis buffer (50 mM Tris-HCl, pH 7.5, 800 mM NaCl, 10% glycerol, 5 mM BME, 10 mM $MgCl_2$, and 0.5% Triton X-100). Cells were lysed via sonication, and RNase A (Sigma-Aldrich #10109169001) was added to a final concentration of 50 µg/mL. The lysate was clarified by centrifugation for 45 minutes at 14,500 rpm and 4 °C. The fusion protein was immobilized on Strep-Tactin Superflow resin (IBA GMBH #2-1208-025), and contaminating proteins and detergent were washed away with extensive washing using wash buffer (20 mM Tris-HCl, pH 7.5, 500 mM NaCl, 10% glycerol, 1 mM DTT). The resin was resuspended, and wild-type A3G-KCK was liberated from the resin by incubating with RNase A and TEV protease for 48 hours at 4 °C under gentle mixing. Following RNase A and TEV digestion, the flow-through was collected, concentrated, and separated on a Superdex SD200 10/300 column in sizing buffer (20 mM Tris, pH 7.5, 500 mM NaCl, 10% glycerol, 1 mM DTT). Fractions corresponding to cleaved dimeric A3G were pooled, concentrated, and separated again on a Superdex SD200 10/300 column. After the second sizing run, fractions corresponding to cleaved dimeric A3G-KCK were pooled and concentrated.

A3G-KCK was labeled with fluorescein-maleimide by combining protein with dye in a 1:1 ratio in the following buffer (20 mM HEPES, pH 7.5, 300 mM NaCl, 0.5 mM TCEP). Protein and dye were incubated at room temperature for 30 minutes and then transferred to 4° C for overnight incubation. Unlabeled dye was removed by desalting using NICK Column Sephadex G-50 DNA grade equilibrated with cold A3G-KCK sizing buffer.

Mass Photometry (MP)

sA3G and VCBC were prepared at 0.5 μM with or without 5 μM RNA20 in the following buffer (25 mM HEPES, pH 7.5, 100 mM NaCl). RNA20 (5'-rCrGrGrUrUrGrArUrCrGrUrUrUrUrArArCrArArA-3') was ordered from IDT. Samples were incubated for at least 20 minutes to allow complex formation. Incubated samples were diluted approximately 1:10 (to a final concentration of ~50 nM) immediately before measurement; the final concentration was then adjusted as needed by adding more sample buffer. The data were collected on a Refeyn OneMP, running AcquireMP software. Calibration was done with BSA, apoferritin, and ADH. Data were analyzed in Refeyn DiscoverMP, using program default settings.

Fluorescence Size Exclusion Chromatography (F-SEC)

In 100-μL reactions, 1 μM of fluorescein-labeled A3G was digested with 2 μL of RNase A/T1 (Thermo Fisher #EN0551) in the following buffer (10 mM Tris-HCl, pH 7.5, 500 mM NaCl, 5 mM EDTA). After incubation, RNase digestion was inhibited with SUPERase • In™ RNase Inhibitor (Fisher Scientific AM2694). 80-μL aliquots were injected and separated on a Superdex SD 200 column at 0.5 mL/min using an FPLC system equipped with a fluorescent detector, with excitation and emission wavelengths set to 488 nm and 508 nm, respectively. Each fluorescence chromatogram was baseline-subtracted, and then the area under the curve was normalized so that the total sum of the areas under each curve equals 1.

$$\text{Absorbance}_{\text{baseline corrected}} = \text{Abs} - \min(\text{Abs})$$

$$\text{Absorbance}_{\text{normalized}} = \frac{\text{Absorbance}_{\text{baseline corrected}}}{\sum \text{Absorbance}_{\text{baseline corrected}}}$$

AUTHOR CONTRIBUTIONS

LAD and JDG conceptualized experiments and analyzed the data. LAD expressed and purified all protein reagents. Gabriel Braun performed Mass Photometry experiments. Wooyoung Choi performed F-SEC experiments.

SUPPLEMENTAL FIGURES

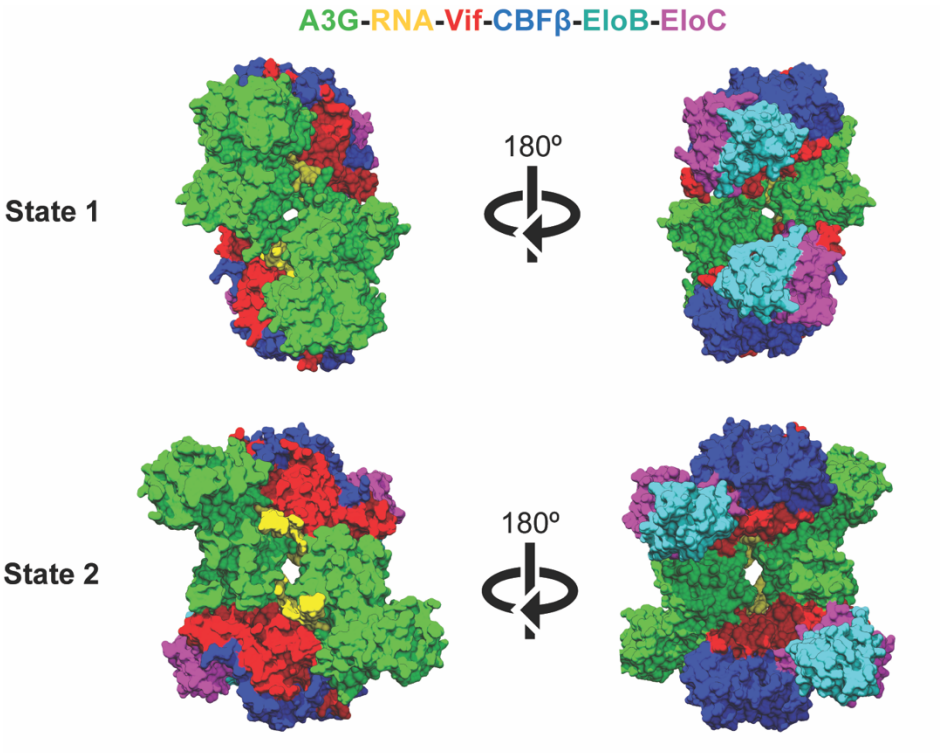

Figure S2.1: Cryo-EM structure of VCBC and A3G dimers on RNA in two configurations. Two copies of VCBC and A3G dimerize on one strand of ssRNA in at least two states based on our Cryo-EM structures. As observed in both states, there is little to no self-association of A3G (red), indicating Vif binds monomeric A3G.

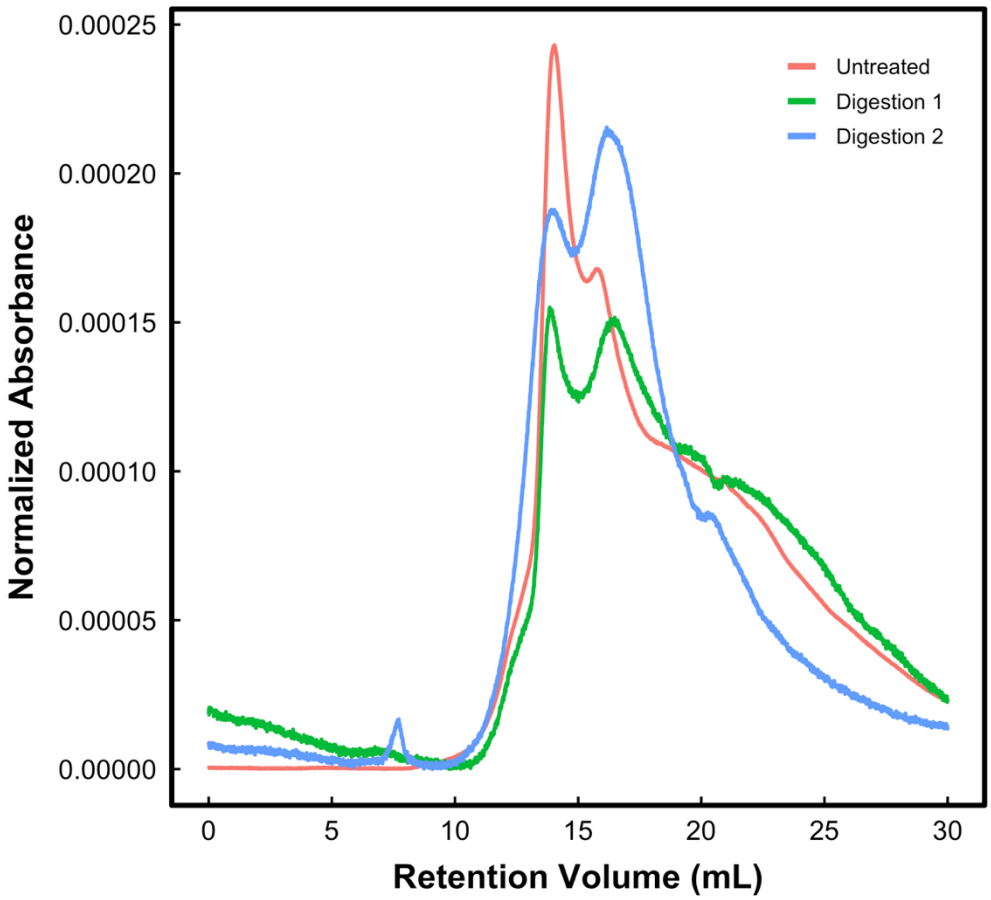

Figure. S2.2: Wild-type A3G digestions with RNase A/T1 for 4 hours. Both digestions were performed in separate experiments. Wild-type A3G was treated with RNase A/T1 for 4 hours on ice and then quenched. Samples were separated on an SD200 column.

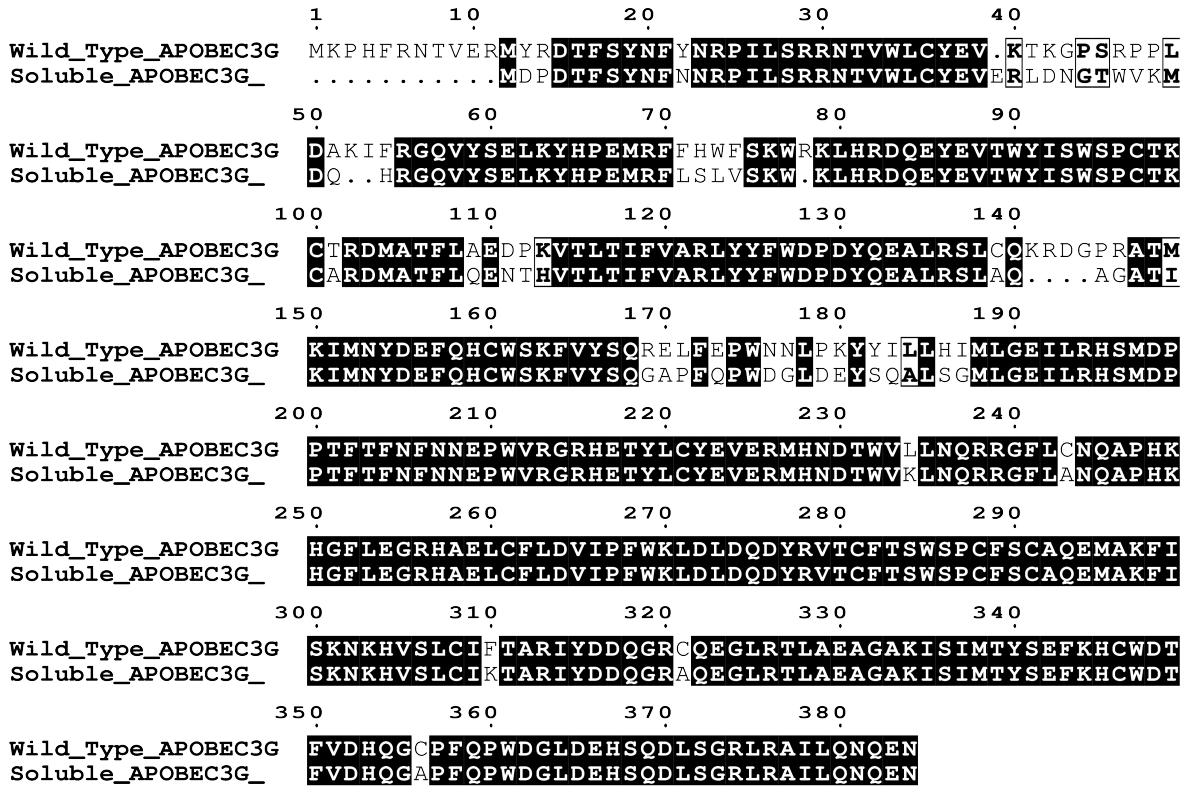

Figure S2.3: Comparison of wild-type A3G and soluble A3G sequences. Sequence of wild-type A3G cloned into the pFASTBAC vector and expressed and purified from Sf9 insect cells. sA3G cloned into the pGEX-6P-1 vector and expressed and purified from bacterial cells.

REFERENCES

1. Barré-Sinoussi, F. *et al.* Isolation of a T-Lymphotropic Retrovirus from a Patient at Risk for Acquired Immune Deficiency Syndrome (AIDS). *Science* **220**, 868–871 (1983).
2. Wain-Hobson, S., Sonigo, P., Danos, O., Cole, S. & Alizon, M. Nucleotide sequence of the AIDS virus, LAV. *Cell* **40**, 9–17 (1985).
3. Sodroski, J. *et al.* Replicative and Cytopathic Potential of HTLV-III/LAV with sor Gene Deletions. *Science* **231**, 1549–1553 (1986).
4. Strebel, K. *et al.* The Hiv A (sor) Gene-product Is Essential For Virus Infectivity. https://hdl.handle.net/2027.42/62702 (1987).
5. Fisher, A. G. *et al.* The sor Gene of HIV-1 Is Required for Efficient Virus Transmission in Vitro. *Science* **237**, 888–893 (1987).
6. Madani, N. & Kabat, D. An Endogenous Inhibitor of Human Immunodeficiency Virus in Human Lymphocytes Is Overcome by the Viral Vif Protein. *J. Virol.* **72**, 10251–10255 (1998).
7. Sheehy, A. M., Gaddis, N. C., Choi, J. D. & Malim, M. H. Isolation of a human gene that inhibits HIV-1 infection and is suppressed by the viral Vif protein. *Nature* **418**, 646–650 (2002).
8. Jarmuz, A. *et al.* An Anthropoid-Specific Locus of Orphan C to U RNA-Editing Enzymes on Chromosome 22. *Genomics* **79**, 285–296 (2002).
9. Harris, R. S. *et* al. DNA Deamination Mediates Innate Immunity to Retroviral Infection. *Cell* **113**, 803–809 (2003).
10. Zhang, H. *et al.* The cytidine deaminase CEM15 induces hypermutation in newly synthesized HIV-1 DNA. *Nature* **424**, 94–98 (2003).
11. Mariani, R. *et al.* Species-Specific Exclusion of APOBEC3G from HIV-1 Virions by Vif. *Cell* **114**, 21–31 (2003).

12. Huthoff, H., Autore, F., Gallois-Montbrun, S., Fraternali, F. & Malim, M. H. RNA-Dependent Oligomerization of APOBEC3G Is Required for Restriction of HIV-1. *PLOS Pathog.* **5**, e1000330–e1000330 (2009).

13. York, A., Kutluay, S. B., Errando, M. & Bieniasz, P. D. The RNA Binding Specificity of Human APOBEC3 Proteins Resembles That of HIV-1 Nucleocapsid. *PLOS Pathog.* **12**, e1005833 (2016).

14. Soros, V. B., Yonemoto, W. & Greene, W. C. Newly Synthesized APOBEC3G Is Incorporated into HIV Virions, Inhibited by HIV RNA, and Subsequently Activated by RNase H. *PLOS Pathog.* **3**, e15 (2007).

15. Li, Y.-L. *et al.* The structural basis for HIV-1 Vif antagonism of human APOBEC3G. *Nature* **615**, 728–733 (2023).

16. Kouno, T. *et al.* Structural insights into RNA bridging between HIV-1 Vif and antiviral factor APOBEC3G. *Nat. Commun.* **14**, 4037 (2023).

17. Asor, R., Loewenthal, D., Wee, R. van, Benesch, J. L. P. & Kukura, P. Mass Photometry. *Annu. Rev. Biophys.* **54**, 379–399 (2025).

18. Simon, J. H. M., Sheehy, A. M., Carpenter, E. A., Fouchier, R. A. M. & Malim, M. H. Mutational Analysis of the Human Immunodeficiency Virus Type 1 Vif Protein. *J. Virol.* **73**, 2675–2681 (1999).

19. Russell, R. A. & Pathak, V. K. Identification of Two Distinct Human Immunodeficiency Virus Type 1 Vif Determinants Critical for Interactions with Human APOBEC3G and APOBEC3F. *J. Virol.* **81**, 8201–8210 (2007).

20. Kouno, T. *et al.* Structure of the Vif-binding domain of the antiviral enzyme APOBEC3G. *Nat. Struct. Mol. Biol.* **22**, 485–491 (2015).

21. Chelico, L., Pham, P., Calabrese, P. & Goodman, M. F. APOBEC3G DNA deaminase acts processively 3′ → 5′ on single-stranded DNA. *Nat. Struct. Mol. Biol.* **13**, 392–399 (2006).

22. Hüttenhain, R. *et al.* ARIH2 Is a Vif-Dependent Regulator of CUL5-Mediated APOBEC3G Degradation in HIV Infection. *Cell Host Microbe* **26**, 86-99.e7 (2019).

CHAPTER 3
APOBEC3G mono-ubiquitination catalyzed by Neddylated CRL5-Vif-CBFβ and ARIH2 is detected by fluorescent ubiquitin

ABSTRACT

RNA promotes HIV-1 Vif binding to sA3G, supporting the hypothesis that RNA is a molecular glue. Based on the structures of Vif bound to A3G, Vif must bind RNA and A3G in a binding mode that properly orients A3G towards the co-enzymes recruited to ubiquitinate A3G. To test whether RNA also promotes A3G ubiquitination, RNA was examined in pulse-chase ubiquitination assays using fluorescent ubiquitin, which monitors the A3G priming step of ubiquitination catalyzed by N8~CRL5-Vif-CBFβ and ARIH2. In the pulse reaction, fluorescent ubiquitin is loaded onto the E2 ubiquitin-conjugating enzyme, UBE2L3, which partners with ARIH2. The chase reaction monitors downstream reactions of UBE2L3~UB formation, specifically as ubiquitin is transferred from UBE2L3 onto ARIH2 and then A3G. The fraction of mono-ubiquitinated A3G can be tracked over time here, allowing us to compare ubiquitination activity under different conditions. RNA's ability to affect sA3G and wild-type A3G mono-ubiquitination was tested here.

INTRODUCTION

Proteins are cleared from cells by the 26S proteasome through the biological process of proteasomal degradation. Proteins are signaled for degradation when acceptor lysine residues have been covalently modified with a chain of Lys48-linked poly-ubiquitin.[1] In a biochemical process known as ubiquitination, ubiquitin is transferred through a series of ubiquitin-activating enzymes in an E1-E2-E3 enzymatic cascade.[2,3] Briefly, UB is activated, and its C-terminal carboxylate is covalently thioester-bonded to an E1 active site cysteine in an ATP-dependent reaction. Next, the E1 transfers UB onto the active site cysteine of an E2-conjugating enzyme. Finally, the thioester-bonded E2 can partner with an E3 ubiquitin ligase, which binds both protein substrate and the E2 conjugating enzyme to transfer ubiquitin to an acceptor lysine residue of the target protein. HIV-1 Vif hijacks an E3 ligase to bind and target A3G for proteasomal degradation.

There are three general classifications of E3 ligases based on their mechanism of ubiquitin transfer, however only two will be reviewed here.[4] Really interesting new gene (RING) E3 ligases catalyze ubiquitin transfer in one step by recruiting the protein substrate and the E2 conjugating enzyme into proximity of one another. These E3 types do not directly accept ubiquitin themselves; instead, they facilitate ubiquitin transfer by recruiting a target protein's acceptor lysine residues in proximity with the thioester-bonded E2 active site loaded with ubiquitin in a zone known as the ubiquitination zone. RING E3s comprise a superfamily of modular E3 ligases known as Cullin RING E3s (CRLs). Vif hijacks the Cullin5 RING E3 ligase (CRL5).

The second type of E3 ligases relevant to this work are RING-between-RING (RBR) family E3s, which catalyze ubiquitin transfer from an E2 conjugating enzyme onto a protein substrate in a two-step process. First, ubiquitin is transferred from the E2 enzyme onto an active site cysteine residue of the RBR E3, and then it is transferred from the RBR E3 onto the protein substrate. ARIH2 is an RBR type E3 ligase, which has been shown to associate with HIV-1 Vif.[5]

Like canonical CRL E3 ligases, the CRL5-Vif-CBFβ ligase recruits ARIH2 to install the first ubiquitin onto A3G, priming it for poly-ubiquitination.[6] This priming step is dependent on covalent modification of the Cullin5 (CUL5) protein with NEDD8, a ubiquitin-like protein.[7] The use of an E3-E3 tag-team mechanism to prime a substrate can be important for ubiquitinating structurally diverse substrates, which may not be accessible by an E2-E3 mechanism alone.[8]

In other words, an E2-E3 mechanism of ubiquitination might not always properly orient acceptor lysine residues of a protein substrate into proximity of a ubiquitin-loaded E2 active site, or the ubiquitination zone. When the neddylated CRL5-Vif-CBFβ E3 ligase is modeled with ARIH2 and A3G, Vif appears to bind A3G and RNA in a manner that properly orients the acceptor lysine residues of A3G towards the ubiquitin-loaded ARIH2 active site (**Fig. 1.2b**).[9] This suggests Vif binds A3G and RNA in a manner that properly orients A3G acceptor lysine residues towards the ubiquitination zone. The relationship between the Vif-RNA-A3G interface and A3G ubiquitination is under investigation here.

In the previous chapter, we demonstrated the successful assembly of Vif-A3G complexes using RNA20. Here, I am interested in determining whether we can observe an RNA-mediated effect on A3G mono-ubiquitination. I hypothesize that, in addition to binding, RNA also plays a significant role in promoting A3G ubiquitination. Using a previously described pulse-chase assay with fluorescently labeled ubiquitin, I study RNA's effect on the priming step of A3G ubiquitination (**Fig. 3.1a**).[10,11] I used this assay to test the role of RNA in promoting A3G mono-ubiquitination with the solubility-optimized A3G variant (sA3G) and wild-type A3G.

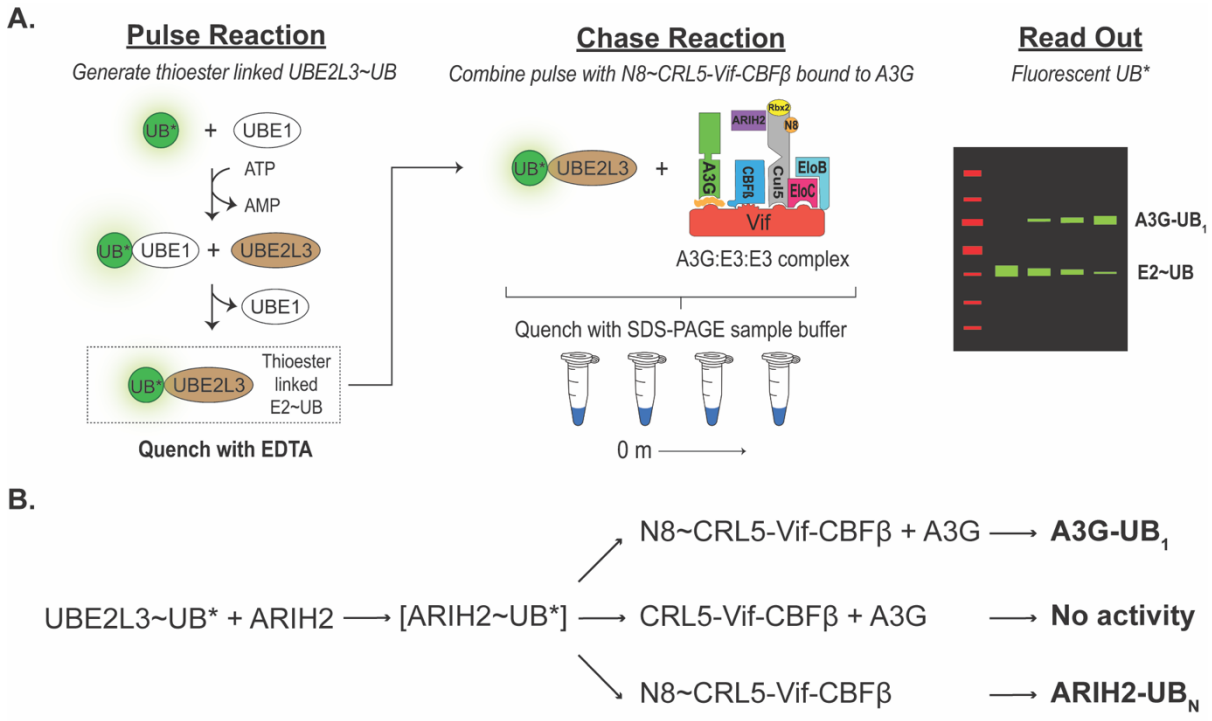

Figure 3.1 Schematic of pulse chase assay to monitor CRL5-Vif-CBFβ and ARIH2 mono-ubiquitination of A3G. A) In the pulse reaction, fluorescent ubiquitin is loaded onto UBE2L3 in an ATP-dependent reaction, and the reaction is quenched with EDTA. An aliquot of the quenched pulse reaction is combined with a pre-incubated mixture of CRL5 incubated with ARIH2 and A3G to initiate the chase reaction. Aliquots of the chase reaction are removed and quenched in SDS-PAGE sample buffer at different time points. Reaction products are separated on an SDS-PAGE gel, and fluorescent ubiquitin is detected on a Typhoon scanner. **B)** Mechanism of reactions downstream of pulse reaction. When substrate is present with a neddylated CUL5 protein, A3G mono-ubiquitination is observed. When the CUL5 is not neddylated, no activity is observed. A certain level of ARIH2 auto-ubiquitination is observed in the presence of the substrate. In the absence of substrate, only Auto-ubiquitination activity is observed.

RESULTS

sA3G mono-ubiquitination is detected but not enhanced by RNA

RNA20 was previously shown to enhance sA3G ubiquitination.[12] I decided to test whether we can also observe this phenomenon using the pulse chase assay described above, with sA3G, RNA20, and the wild-type CRL5-Vif-CBFβ E3 ligase. The formation of mono-ubiquitinated sA3G is detected over 30 minutes using the pulse chase assay (**Fig. 3.2a, gel 1**). This process is also neddylation dependent as sA3G mono-ubiquitination is not observed when the chase reaction is performed with C5L5-VCBC-CBFβ that has not been neddylated (**Fig. 3.2a, gel 2**), which serves as a negative control. Since some level of ARIH2 self-modification is expected, the chase reaction was also run without any sA3G present, allowing bands correlating to different ubiquitinated species to be identified (**Fig. 3.2a, gel 3**). Treating UBE2L3~UB* as the starting material and A3G-UB_1 as the final product, we can use their band intensities to quantify the fraction of A3G ubiquitinated over 30 minutes (**Fig. 3.2b**). With our functional pulse chase ubiquitination assay, I aimed to investigate whether we could observe a decrease in the activity of sA3G mono-ubiquitination when RNA20 is removed from the reaction (**Fig. 3.3**).

sA3G poly-ubiquitination was previously observed in the absence of RNA20, though it is not ubiquitinated to a comparable level when RNA20 is present.[12] Therefore, a decrease in sA3G ubiquitination activity is expected. When RNA20 is removed from chase reactions, sA3G mono-ubiquitination is still observed (**Fig. 3.3a, gel 3**). Although based on the fraction ubiquitinated, it appears that sA3G mono-ubiquitination is still observed at the same level as when RNA20 is present (**Fig. 3.3b**). This suggests that RNA does not affect sA3G ubiquitination. This contrasts with what was previously reported and what we observed in our molecular glue assay (**Fig. 2.1**). This discrepancy could be attributed to differences in concentrations, as well as variations in how the different ubiquitination assays are conducted. Since the H43A/Y44A Vif mutation impaired binding to sA3G, I decided to see if sA3G mono-ubiquitination could also be abolished with this mutation (**Fig. 3.4**).

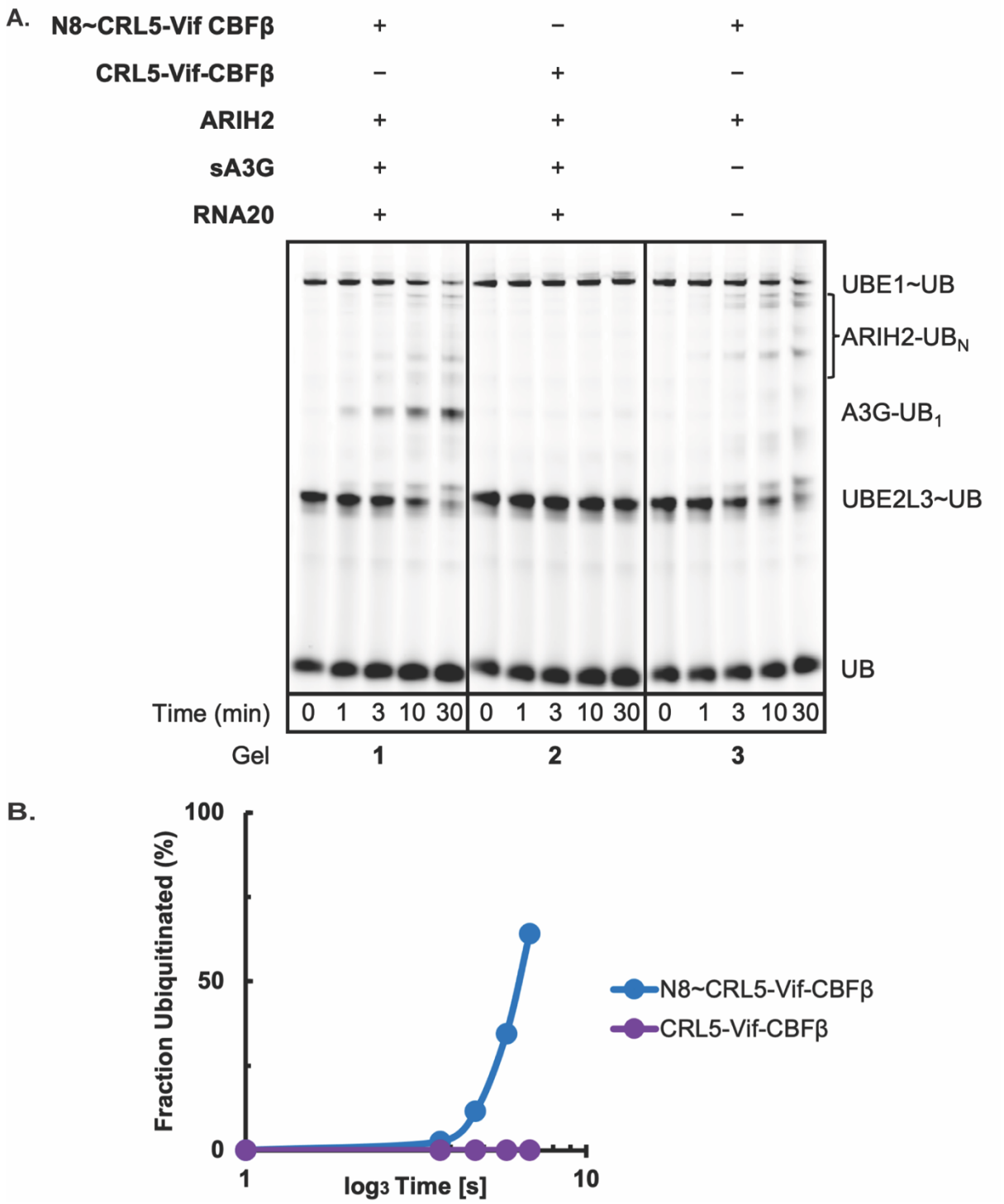

Figure 3.2: Chase Reactions with N8~CRL5-Vif-CBFβ and sA3G. **A)** Reaction products were separated on an SDS-PAGE gel, and fluorescent ubiquitin was detected by scanning gels on an Amersham Typhoon. Each gel is a different chase reaction. Gel 1 is a positive control. Gel 2 was run with CRL5-Vif-CBFβ with a Cullin that has not been neddylated, serving as a negative control. Gel 3 does not contain sA3G, ARIH2 auto-ubiquitination is detected. **B**) Intensities of UBE2L3~UB and sA3G-UB_1 are used to quantify Fraction Ubiquitinated (%) by taking sA3G-UB_1 over the sum of UBE2L3~UB and sA3G-UB_1.

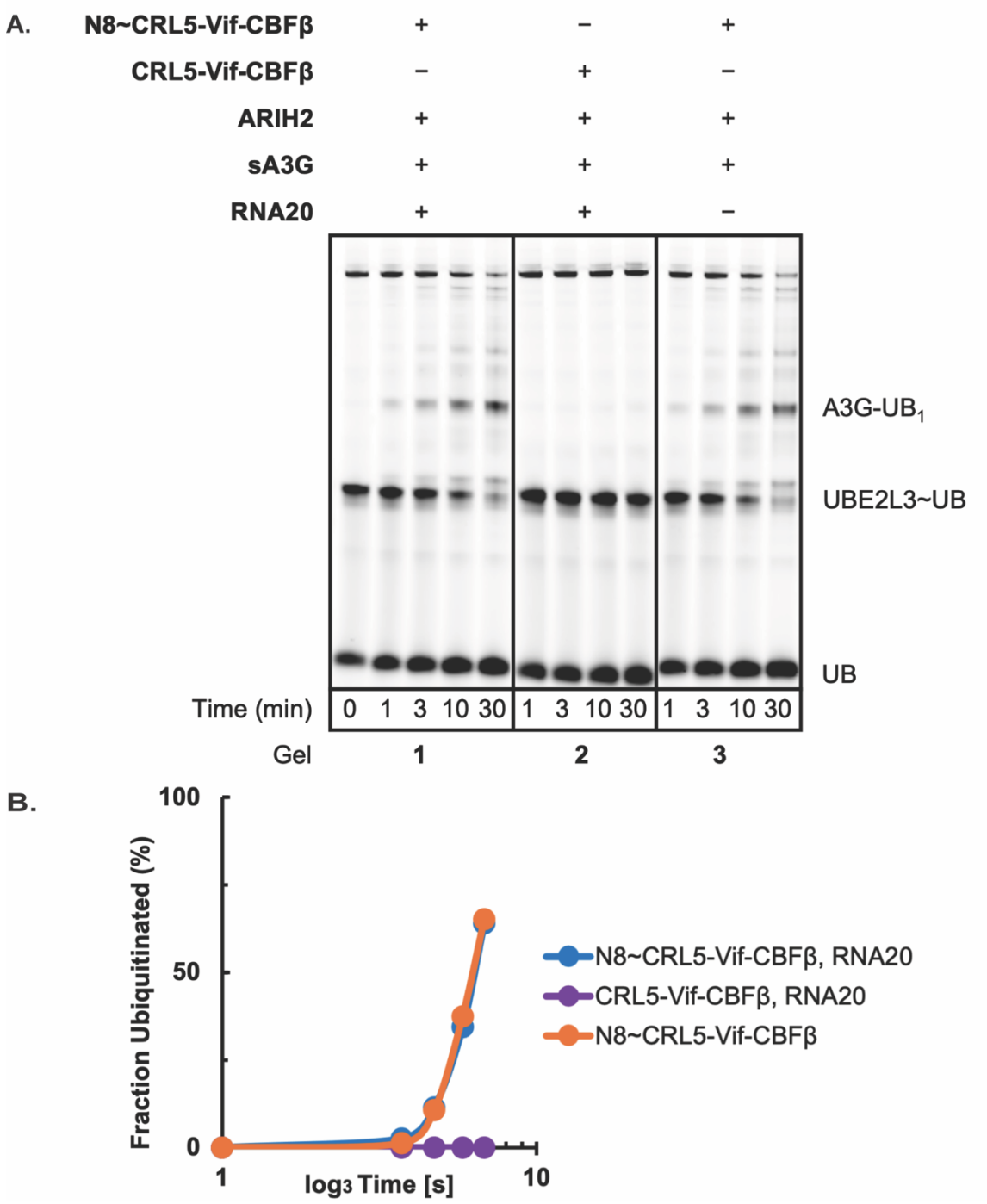

Figure 3.3: RNA20 does not affect sA3G ubiquitination. A) Fluorescent scans of Chase Reactions comparing sA3G ubiquitination in the presence or absence of RNA20. The zero-time point contains only the components of the pulse reaction, since all chase reactions are initiated from the same pulse reaction, I only showed the zero-time point for one reaction. **B)** The addition of RNA20 does not have any impact on sA3G mono-ubiquitination.

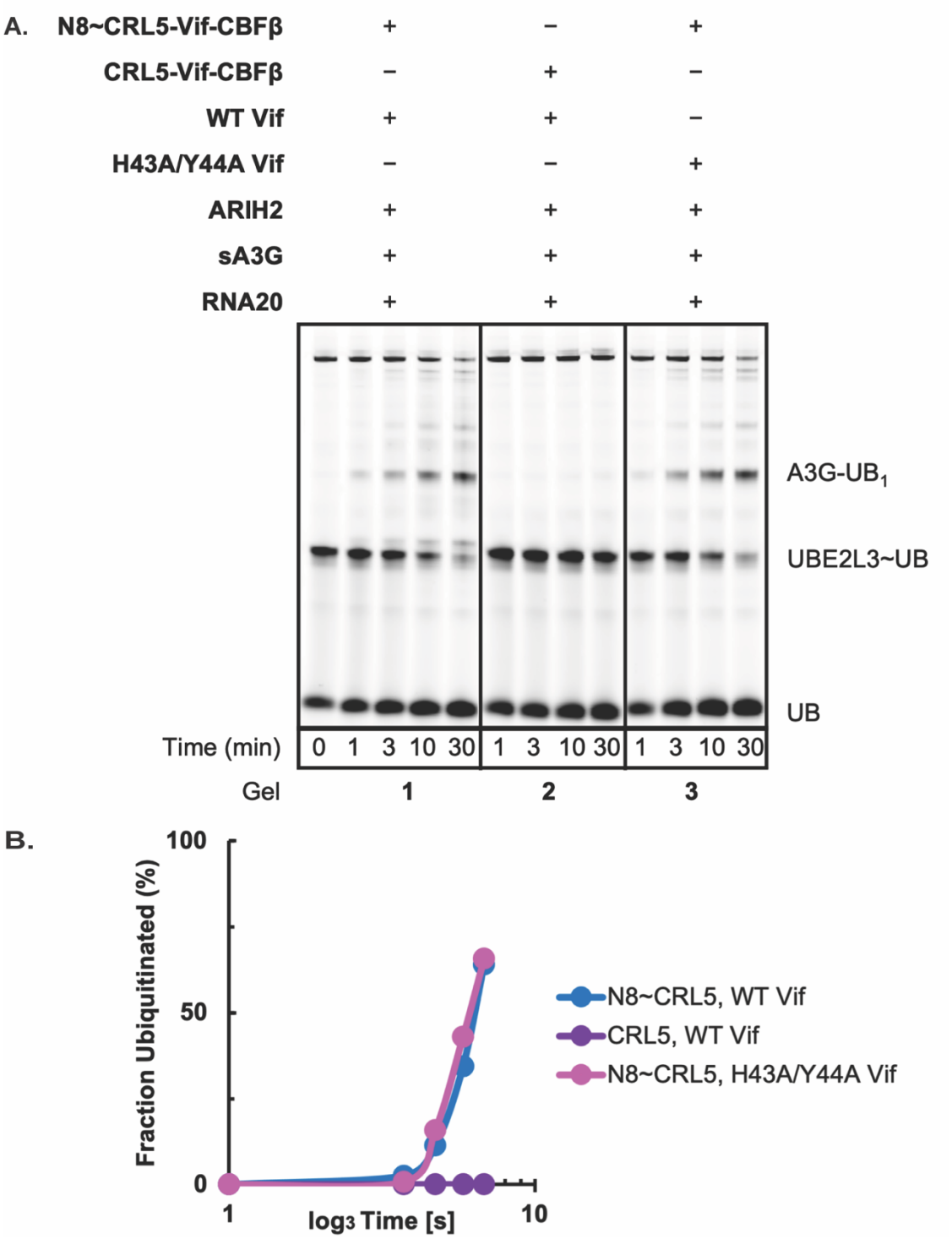

Figure 3.4: Testing sA3G mono-ubiquitination with Vif double-alanine mutation. A) Fluorescent scans of Chase Reaction products. Only the zero time point is shown for gel 1. **B)** H43A/Y44A does not have any effect on the fraction of sA3G mono-ubiquitinated over 30 minutes.

A previous study using sA3G employed a similar double alanine mutation at positions H42 and H43 of Vif, which was shown to abolish the degradation of sA3G in cells, suggesting that Vif is unable to bind and ubiquitinate sA3G.[12] H42 of Vif binds to RNA directly, whereas H43 and Y44 exclusively bind both RNA and A3G. Since we observed no binding between H43A/Y44A Vif and sA3G, we expect it should be unable to mono-ubiquitinate sA3G. Unexpectedly, N8~CRL5-Vif-CBFβ E3 ligases mono-ubiquitinated sA3G (**Fig. 3.4a, gel 3**). Neddylated CRL5 E3 ligases that contained the H43A/Y44A Vif mutation mono-ubiquitinated sA3G at the same level as the wild-type E3 ubiquitin ligase (**Fig. 3.4b**). Since the mutations were not at positions H42 and H43, this might explain why we did not observe a decrease in ubiquitination activity. However, that does not explain the difference in function when binding sA3G.

The most likely explanation is that ubiquitination and RNA binding assays were conducted at different concentrations of Vif and sA3G, which could explain the discrepancy in some of the data. Specifically, why is an RNA-mediated effect on sA3G binding observed but not mono-ubiquitination? Similarly, why is the H43A/Y44A Vif mutation unable to bind sA3G in our binding assays but retains the ability to mono-ubiquitinate sA3G? The ubiquitination assays may be run at a sA3G concentration that binds Vif independent of RNA. An idea that will be discussed in more detail. Currently, it appears RNA does not affect sA3G ubiquitination. Since the wild-type A3G copurifies with RNA, I also wanted to test whether the mono-ubiquitination of wild-type A3G could be disrupted by RNase A/T1 treatment.

RNase A/T1 treatment of wild-type A3G does not affect mono-ubiquitination

The pulse chase assay can also detect wild type A3G mono-ubiquitination catalyzed by N8~CRL5-Vif-CBFβ and ARIH2 (**Fig. 3.5**). As we observed in Chapter 2 in our F-SEC experiments, RNase A/T1 treatment of wild type A3G can partially convert dimeric A3G to A3G monomer (**Fig. 2.3, Fig. S2.2**). This could be attributed to the degradation of copurified RNA between wild-type A3G dimers. Based on that assumption and to test whether RNA promotes

wild-type A3G ubiquitination, I treated the samples with RNase A/T1 before running the chase reaction. One might expect mono-ubiquitination to be disrupted. It is essential to note that wild-type A3G is digested with RNase A/T1 in a buffer with NaCl concentrations that exceed the concentration at which the chase reaction is conducted, 100 mM NaCl. I decided to try the chase reaction with wild-type A3G in a gradient of NaCl concentrations (**Fig. 3.6**).

At 300 mM NaCl, wild-type A3G mono-ubiquitination is decreased, which is expected (**Figure 3.6, gel 3**). However, this does not appear to be RNAse A/T1-dependent and may be due to the high salt concentration at which these reactions were conducted (**Figure 3.6, gel 4**). At 500 mM NaCl, the concentration at which F-SEC experiments are performed, A3G mono-ubiquitination also decreases, but does not appear to be RNase A/T1-dependent (**Fig. 3.6, gels 5 and 6**). The high salt concentration also seems to inhibit the chase reaction, as indicated by a rapid decrease in the levels of UBE2L2~UB at earlier time points (**Fig. 3.6**, **gels 3-6**). Even if wild-type A3G is digested with RNase A/T1 at a NaCl concentration similar to that of the chase reactions, no decrease in mono-ubiquitinated A3G is observed (**Fig. S3.1**).

Assessing the role of RNA in binding and ubiquitination experiments with wild-type A3G is currently challenging due to various reasons related to co-purified RNA. These include the inability to generate an RNA-free monomeric sample to use in binding assays. Here, it appears that the high concentration of salt in which RNase A/T1 digestions occur negatively affects the overall ubiquitination assay. While this pulse chase assay can be used to monitor wild-type A3G mono-ubiquitination catalyzed by N8~CRL5-Vif-CBFβ and ARIH2 successfully, these issues must be carefully addressed before further examining the relationship between Vif-RNA-A3G binding and A3G ubiquitination.

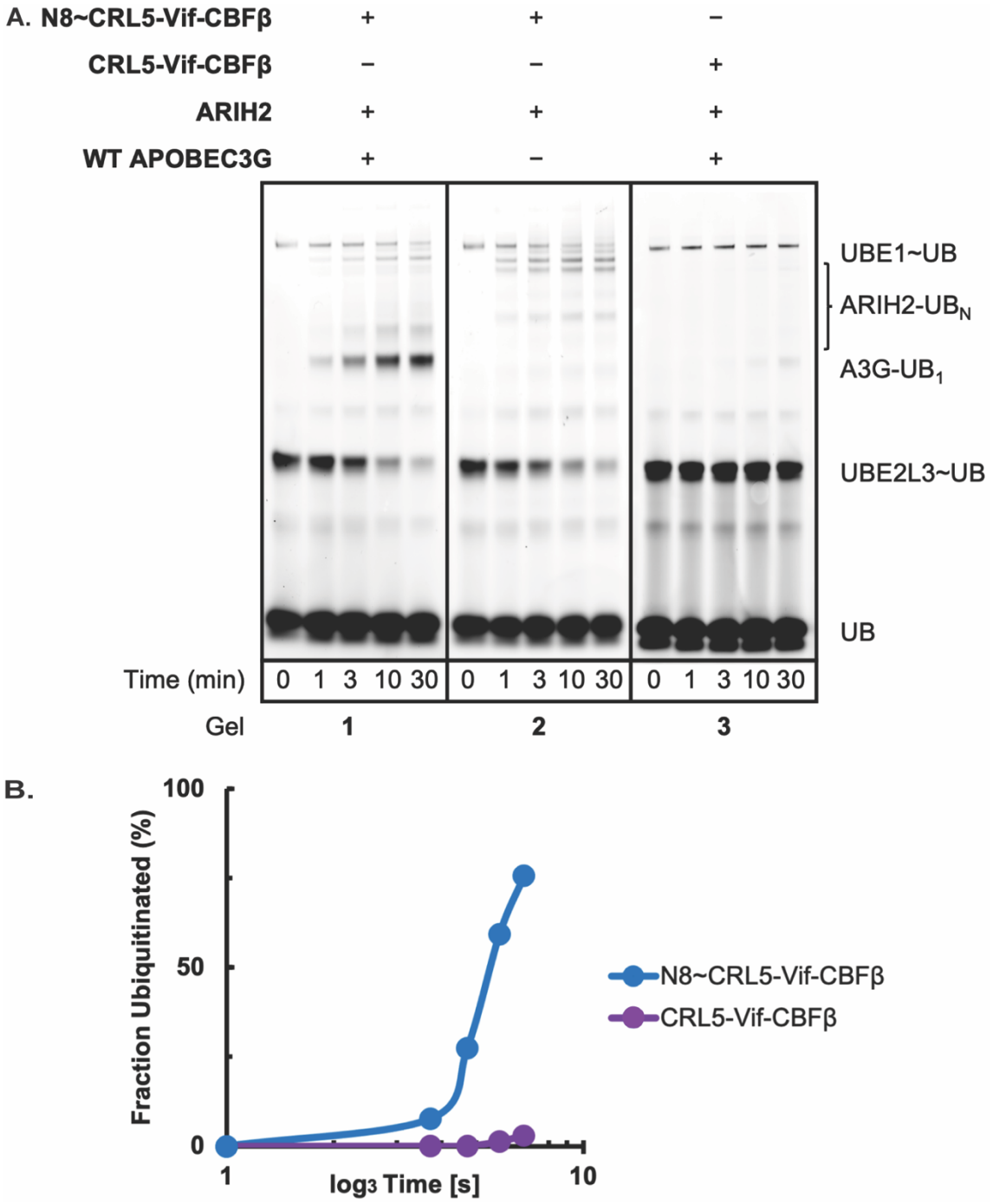

Figure 3.5: Chase Reaction with N8~CRL5-Vlf-CBFβ and wild type A3G A) Fluorescent scans of products from Chase Reactions with N8~CRL5-Vif-CBFβ and wild type A3G. **B**) Intensities of UBE2L3~UB and wild-type A3G-UB$_1$ are used to quantify Fraction Ubiquitinated (%) by taking wild-type A3G-UB$_1$ over the sum of UBE2L3~UB and wild-type A3G-UB$_1$.

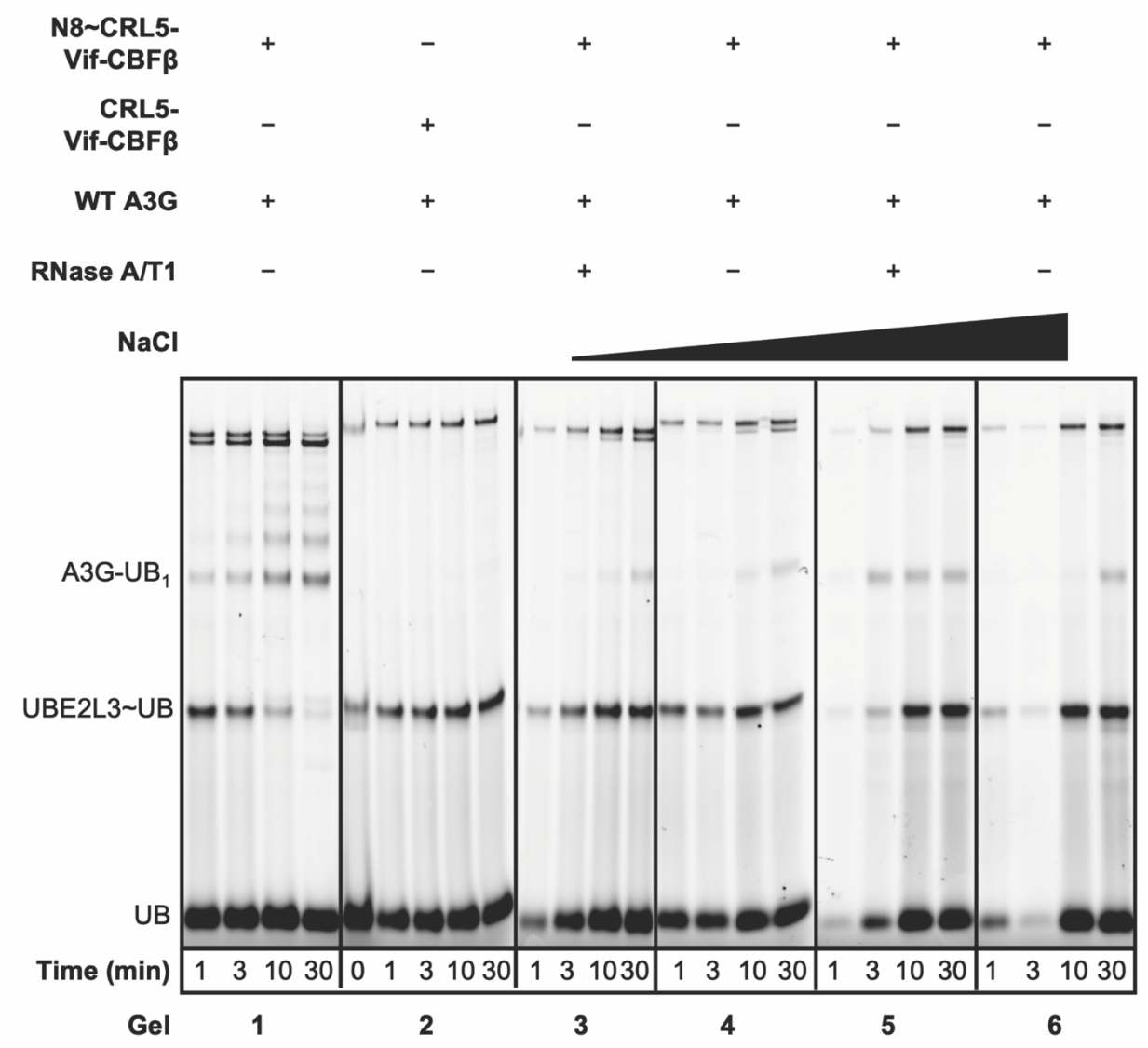

Figure 3.6: Testing RNase A/T1 digested wild-type A3G in chase reactions with salt titration. A) Fluorescent scans of products from Chase Reactions with N8~CRL5-Vif-CBFβ and wild-type A3G that is RNase A/T1 digested at different NaCl concentrations. A3G was digested in chase buffer with either 300 mM (Gel 3-4) or 500 mM NaCl (Gel 5-6). The NaCl concentrations were further diluted in the actual chase reaction to ~212 mM and 330 mM.

DISCUSSION

Previously, we demonstrated that RNA is a molecular glue that promotes HIV-1 Vif binding to sA3G. Here, I was interested in determining whether a similar effect could be observed with A3G mono-ubiquitination catalyzed by N8~CRL5-Vif-CBFβ and ARIH2. I used a pulse chase assay which utilizes fluorescent ubiquitin to monitor mono-ubiquitination of sA3G (**Fig. 3.2**). While the assay is successful in detecting sA3G mono-ubiquitination, we were unable to observe an RNA-mediated effect on sA3G mono-ubiquitination (**Fig. 3.3**). Likewise, even using the H43A/Y44A Vif mutation, which we previously demonstrated abolishes binding between Vif, RNA20, and sA3G, we observed no effect on sA3G mono-ubiquitination (**Fig. 3.4**). We suspect that the discrepancy between an RNA-mediated effect on HIV-1 Vif-sA3G binding versus sA3G mono-ubiquitination is likely attributed to a difference in protein concentrations.

Our molecular glue assay is conducted at sub-micromolar concentrations where both sA3G and VCBC are combined at an equimolar concentration of ~50 nM. Whereas in our ubiquitination assays, sA3G and VCBC are combined in a 1:10 molar ratio, respectively. By the chase reactions, Vif is diluted to 400 nM, while sA3G is diluted to 4 μM. Our ubiquitination assays are likely being conducted at a concentration of sA3G that far exceeds any RNA-mediated effect on sA3G-VCBC assembly. This could help explain why 1) removing RNA20 and 2) using the H43A/Y44A Vif mutant are unable to abolish sA3G mono-ubiquitination. The use of fluorescent ubiquitin hinders the lower limit of detection, as we can only lower the concentration of sA3G to 1 μM before we lose signal of mono-ubiquitinated sA3G.

As we will discuss more in Chapter 4, more sensitive detection methods should be employed to determine if the concentration in which these experiments are conducted matters. This is likely due to the differences in results between the binding and ubiquitination experiments, as well as the differences in concentrations at which both experiments were conducted. Regardless, the ability to monitor and quantify A3G mono-ubiquitination is a

success. The ubiquitination assay not only detects sA3G mono-ubiquitination but also successfully monitors wild-type A3G mono-ubiquitination (**Fig. 3.5**).

In this chapter, we present an assay to assess and quantify mono-ubiquitination of A3G catalyzed by N8~CRL5-Vif-CBFβ and ARIH2 using fluorescent ubiquitin. While not reported here, this pulse chase assay can be further adapted to monitor priming and extension of the poly-ubiquitination chain catalyzed by N8~CRL5-Vif-CBFβ.[10] This work also serves as a building block for expanding our ability to carefully interrogate the relationship between Vif-RNA-A3G binding and A3G ubiquitination. Further work is needed to demonstrate the role RNA plays in promoting the ubiquitination of A3G. Enzyme kinetics have not been conducted on A3G ubiquitination before, this assay can be further developed to obtain kinetic parameters such as K_m and V_{max}. Such constants could reveal additional biochemical requirements for Vif-mediated ubiquitination that extend beyond a simple binding model.

METHODS

Plasmids

Plasmids encoding ubiquitin E1 (UBE1), UBE2L3, Cul5/RBX2, ARIH2, NEDD8 E1 (APPBP1-UBA3), NEDD8 E2, and NEDD8 were prepared and purified as previously described.[5] VCBC, mutant VCBC, sA3G, and wild-type A3G (with no KCK tag) were cloned and purified as described in Chapter 2. To generate fluorescent ubiquitin, an N-terminal PKA site with the acceptor serine residue altered to cysteine was cloned into a pGEX-2TK vector.

Protein Expression and Purification

ARIH2 was purified from BL21 (DE3) cells transformed with pGEX4T1 GST-ARIH2. Cells were grown in LB media to an OD of ~0.6 at 37° C before being induced with 0.1 mM IPTG and 0.1 mM $ZnCl_2$. After induction, the cells were grown at 16° C overnight. Cells were pelleted at 4000 rpm for 20 minutes at 4 °C and immediately lysed in the following lysis buffer: 20 mM HEPES (pH 8), 50 mM NaCl, 0.1 mM $ZnCl_2$, and 1 mM DTT. The lysate was clarified by centrifugation for 40 minutes at 4 °C and 14,500 rpm. Clarified lysate was loaded onto a GST column (Cytiva #17513101) and washed with ARIH2 GST Buffer A (20 mM HEPES pH 8, 500 mM NaCl, 0.1 mM $ZnCl_2$, and 1 mM DTT). GST ARIH2 was eluted from the column on a FPLC using a gradient elution with ARIH2 GST Buffer B (20 mM HEPES pH 8, 500 mM NaCl, 40 mM reduced glutathione, 0.1 mM $ZnCl_2$, and 1 mM DTT). Peaks correlating to GST ARIH2 were pooled and reduced glutathione was desalted using ARIH2 GST Buffer A and PD-10 Desalting Columns with Sephadex G-25 Resin (Cytiva #17-0851-01). Thrombin (Cytiva #27-0846-01) was added to the desalted fraction, and the digestion was performed overnight at 4 °C. Following overnight incubation, the digestion was back-passed over the GST column, and the flow-through was collected and concentrated. The concentrated backpass was loaded onto an SD200 column equilibrated with ARIH2 sizing buffer (25 mM HEPES, pH 8, 200 mM NaCl, 0.1 mM $ZnCl_2$, and 1 mM DTT). SEC fractions were pooled and concentrated.

Fluorescent human ubiquitin was generated by transforming BL21 (DE3) cells with the

pGEX-2TK vector encoding UB with an N-terminal (S->C) PKA site. Cells were grown at 37° C to an OD of ~0.6 and induced with 0.6 mM IPTG, followed by overnight growth at 16° C. Cells were pelleted by centrifugation at 4000 rpm for 20 minutes at 4° C. Cells were resuspended and lysed by sonication in the following lysis buffer (50 mM Tris-HCl pH 7.5, 200 mM NaCl, 5 mM DTT). The lysate was clarified by centrifugation at 14,500 rpm for 40 minutes at 4° C. Clarified lysate was loaded onto Glutathione Sepharose™ 4B resin (Cytiva #17-0756-01) pre-equilibrated with the lysis buffer. The resin was washed with the same buffer, and GST-UB was eluted with the following buffer: 50 mM Tris-HCl (pH 7.5), 200 mM NaCl, 10 mM reduced glutathione, and 1 mM DTT. Glutathione was removed by dialysis with SEC buffer (25 mM HEPES, pH 7.5, 200 mM NaCl, 1 MM DTT) and thrombin to cleave overnight at 4° C. The cleaved fraction was concentrated down and separated on a s75 column pre-equilibrated with SEC buffer. Fractions correlating to UB were pooled, and the concentration was determined using a BSA assay.

The protein was fluorescently labeled as described before.[10] Briefly, UB was diluted to 500 μM in the following labeling buffer: 25 mM HEPES (pH 7.5), 200 mM NaCl. 10 mM DTT was added to reduce the cysteine residue on the PKA site. Excess DTT was removed by desalting with a NAP-5 buffer exchange column (Cytiva #17-0853-01), which was equilibrated with the labeling buffer. The UB concentration was determined by UV-VIS spectroscopy, and 7 molar excess of fluorescein-maleimide was added. The protein-dye mixture was incubated at room temperature for 2 hours and then transferred to 4 °C overnight. The labeling reaction was quenched with 10 mM DTT and incubated on ice for 20 minutes. Excess dye was initially desalted using a PD-10 column, followed by separation on an S75 column pre-equilibrated with sizing buffer. Fluorescent ubiquitin was quantified and aliquoted.

Neddylated Cul5:RBX2 was generated by combining the following components: 1 mg/mL BSA, 4 μM Cul5:RBX2, 2 mM ATP, 0.5 μM NEDD8 E1, 2 μM NEDD8 E2 (UBE2F), and 30 μM NEDD8 in the following buffer (50 mM Tris HCl, pH 7, 50 mM NaCl, 2.5 mM $MgCl_2$). The reaction was run overnight at 4° C. The reaction is separated on a 1-mL HiTrap Heparin HP

column (Cytiva #17-0406-01), pre-equilibrated in N8 Buffer A (20 mM HEPES, pH 8, 300 mM NaCl, 10% glycerol, 1 mM DTT). Neddylated Cul5-RBX2 is eluted from the 1-mL Heparin column using a gradient elution with N8 Buffer B (20 mM HEPES pH 8, 1000 mM NaCl, 10% glycerol, 1 mM DTT). Fractions correlating to eluted neddylated Cul5-RBX2 are pooled and separated on an SD200 column equilibrated in N8 Buffer A. Fractions from SEC correlating to neddylated Cul5:RBX2 are pooled and concentrated.

Pulse Chase Assay

Generally, pulse chase assays are done in the following order: 1) Form N8~CRL5-Vif-CBFβ (positive) and CRL5-Vif-CBFβ (negative) E3 complexes, 2) Generate E3:E3:A3G complexes, 3) Pulse reaction, 4) Chase Reactions. N8~CRL5-Vif-CBFβ is made by simply combining N8~Cul5-RBX2 and VCBC at a final concentration of 4 μM each in 1X Chase Buffer (25 mM HEPES, pH 7.5, 100 mM NaCl), incubating at room temperature for 30 minutes, and then transferring to ice. The negative control is made with Cul5:RBX2, not N8-Cul5:RBX2. E3:E3:A3G complexes are generated in separate tubes as Pre-Initiation mixtures by combining 1 μM CRL5-Vif-CBFβ E3 ligase from step 1, 0.25 μM ARIH2, 10 μM A3G, and 20 μM RNA20. Pre-initiation mixtures are incubated on ice for 20 minutes and transferred to room temperature for at least 5 minutes before use in chase reactions.

The pulse reaction is generated by combining 1.2 μM UbE1, 4 μM UBE2L3, 12 μM fluorescent UB in 1X loading buffer (25 mM HEPES pH 7.5, 100 mM NaCl, 2.5 mM $MgCl_2$, and 1 mM ATP). 6 μL of Pulse Reaction will be required per Chase Reaction, adjust final volume accordingly. Pulse reaction is initiated by the addition of fluorescent UB and is run for 25 minutes at room temperature. The pulse reaction has been optimized so that ~100% of free UBE2L3 is converted to UBE2L3~UB*. The pulse reaction is quenched by the addition of 5 mM EDTA and then incubated on ice, remaining stable for up to 30 minutes.

In a separate tube labeled Chase Reaction, 30 μL of 1X Chase Buffer is aliquoted. One chase reaction tube is made up per Pre-Initiation mix from step 2. Five quench tubes are

prepared, with 14 µL of 2X Non-reducing SDS Sample Buffer (Bioworld #21420019-1) aliquoted into the first tube for $T_{0.}$ 7 µL of 2X NR SDS sample buffer is aliquoted to the following four time points. 6 µL of the quenched pulse reaction is added to the 30 µL in the Chase Reaction tube for a final volume of 36 µL. Gently mix by pipetting up and down, and remove 6 µL to bring the volume back to 30 µL. Add 14 µL of 2X NR SDS sample buffer to the T0 quench tube. The Chase Reaction is initiated by adding 20 µL of the pre-initiation mixture to the 30 µL in the Chase Reaction tube, which contains the diluted pulse reaction. 7 µL aliquots are removed and quenched at various time points.

The final concentration of components is: 0.4 µM UBE2L3~UB (assuming 100% conversion), 0.1 µM ARIH2, 4 µM A3G, and 0.4 µM N8~CRL5-Vif-CBFβ. T_0 should only be the pulse reaction. Reaction products from quench tubes are separated on an SDS-PAGE by gel electrophoresis; there is no need to boil the sample. The gel is imaged on an Amersham Typhoon with Cy2 to detect fluorescein-labeled ubiquitin. If using PageRuler Plus Prestained 10 250 kDa Protein Ladder (Thermo Scientific #26619), a short IR scan can also be run to detect the ladder. Approximate molecular weights are: Ubiquitin = 9 kDa, UBE2L3~UB = 27 kDa, A3G-UB_1 = 59 kDa.

For Chase Reactions with wild type A3G and RNase A/T1 digestions, wild type A3G was digested with RNase A/T1 (Thermo Fisher #EN0551) at 20 µL RNase A/T1 / 1 mL reaction in Chase Buffer with 5 mM EDTA and NaCl concentrations of either 100 mM NaCl, 300 mM NaCl, or 500 mM NaCl for 4 hours on ice. RNase A/T1 digestions were quenched with SUPERase • In™ RNase Inhibitor (Fisher Scientific AM2694) before the addition of neddylated or non-neddylated CRL5-Vif-CBFβ and ARIH2 to generate Pre-Initiation mixtures.

AUTHOR CONTRIBUTIONS

LAD and JDG conceptualized experiments and analyzed the data. LAD expressed and purified protein reagents and conducted pulse chase assays.

SUPPLEMENTAL FIGURES

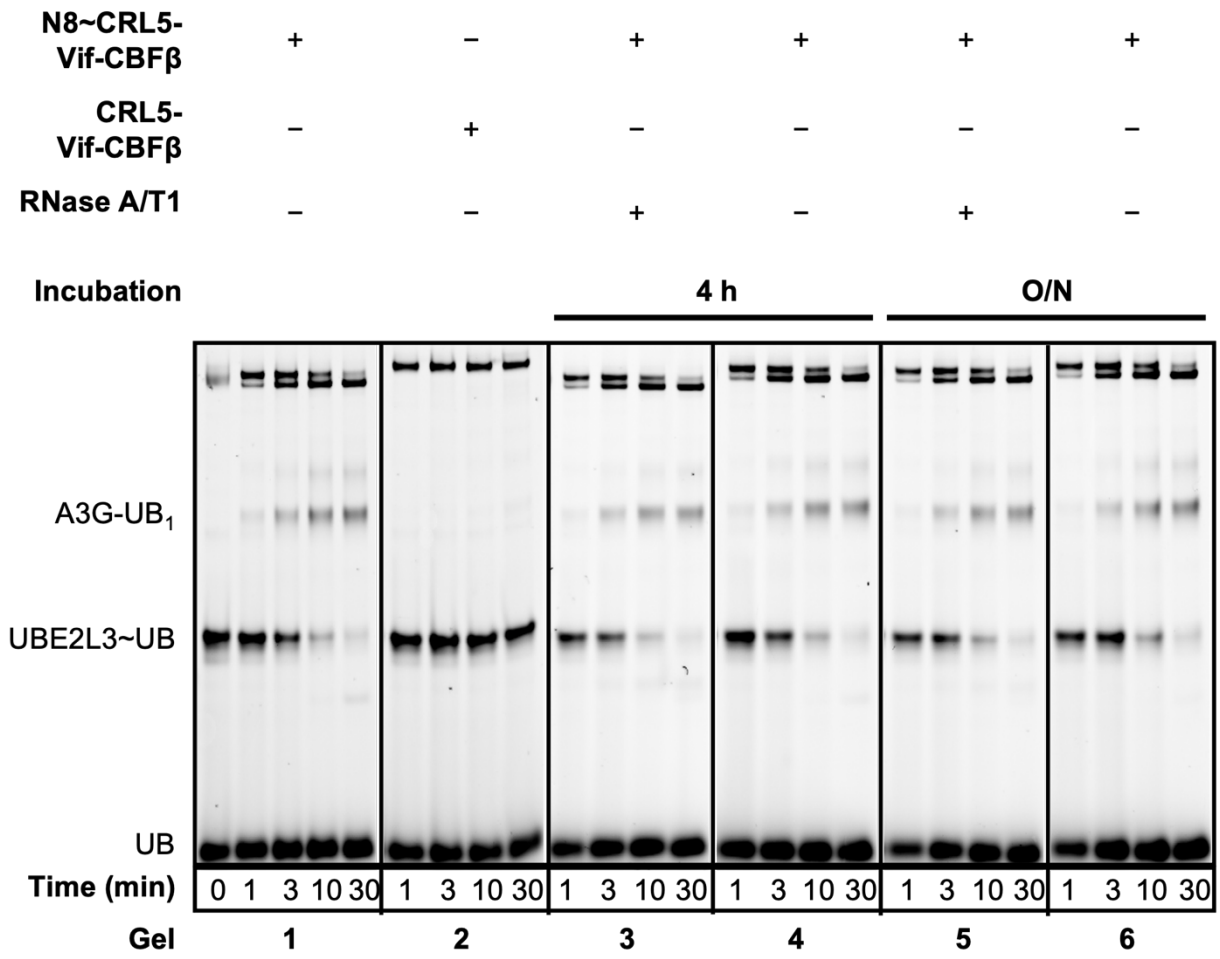

Figure S3.1: Testing RNase A/T1 digestion in normal chase reactions. A) Fluorescent scans of products from Chase Reactions with N8~CRL5-Vif-CBFβ and wild-type A3G that is RNase A/T1 digested in normal 1X Chase Buffer. A3G was digested with RNase A/T1 for either 4 hours (Gel 3) or overnight (Gel 5). Following RNase A/T1 digestion, A3G was combined with N8~CRL5-Vif-CBFβ and ARIH2 in the pre-initiation mixture.

REFERENCES

1. Thrower, J. S., Hoffman, L., Rechsteiner, M. & Pickart, C. M. Recognition of the polyubiquitin proteolytic signal. *EMBO J.* **19**, 94–102 (2000).
2. Hershko, A., Ciechanover, A., Heller, H., Haas, A. L. & Rose, I. A. Proposed role of ATP in protein breakdown: conjugation of protein with multiple chains of the polypeptide of ATP-dependent proteolysis. *Proc. Natl. Acad. Sci.* **77**, 1783–1786 (1980).
3. Ciechanover, A., Heller, H., Elias, S., Haas, A. L. & Hershko, A. ATP-dependent conjugation of reticulocyte proteins with the polypeptide required for protein degradation. *Proc. Natl. Acad. Sci.* **77**, 1365–1368 (1980).
4. Berndsen, C. E. & Wolberger, C. New insights into ubiquitin E3 ligase mechanism. *Nat. Struct. Mol. Biol.* **21**, 301–307 (2014).
5. Hüttenhain, R. *et al.* ARIH2 Is a Vif-Dependent Regulator of CUL5-Mediated APOBEC3G Degradation in HIV Infection. *Cell Host Microbe* **26**, 86-99.e7 (2019).
6. Scott, D. C. *et al.* Two Distinct Types of E3 Ligases Work in Unison to Regulate Substrate Ubiquitylation. *Cell* **166**, 1198-1214.e24 (2016).
7. Kelsall, I. R. *et al.* TRIAD1 and HHARI bind to and are activated by distinct neddylated Cullin-RING ligase complexes. *EMBO J.* **32**, 2848–2860 (2013).
8. Horn-Ghetko, D. *et al.* Ubiquitin ligation to F-box protein targets by SCF–RBR E3–E3 super-assembly. *Nature* **590**, 671–676 (2021).
9. Li, Y.-L. *et al.* The structural basis for HIV-1 Vif antagonism of human APOBEC3G. *Nature* **615**, 728–733 (2023).
10. Scott, D. C. & Schulman, B. A. Chapter Two - Dual-color pulse-chase ubiquitination assays to simultaneously monitor substrate priming and extension. in *Methods in Enzymology* (ed. Hochstrasser, M.) vol. 618 29–48 (Academic Press, 2019).
11. Kostrhon, S. *et al.* CUL5-ARIH2 E3-E3 ubiquitin ligase structure reveals cullin-specific NEDD8 activation. *Nat. Chem. Biol.* **17**, 1075–1083 (2021).

12. Kouno, T. *et al.* Structural insights into RNA bridging between HIV-1 Vif and antiviral factor APOBEC3G. *Nat. Commun.* **14**, 4037 (2023).

Chapter 4

FUTURE DIRECTIONS

In this work, the role of RNA was assessed in promoting Vif-A3G binding, as well as in facilitating A3G mono-ubiquitination catalyzed by the CRL-Vif-CBFβ E3 ubiquitin ligase. In the molecular glue assay described in Chapter 2, RNA-mediated assembly of a complex between sA3G and VCBC is observed (**Fig. 2.1**). This functional assay is validated when using a double-alanine mutation of Vif at positions H43 and Y44, which abolishes the interaction between Vif and sA3G and RNA20 (**Fig. 2.2**). This work supports the hypothesis that RNA is a molecular glue, demonstrating its importance in promoting Vif-A3G binding. The role of RNA was then tested in promoting A3G ubiquitination.

Vif ubiquitinates A3G in two steps, first by priming A3G by installing a terminal ubiquitin, followed by extension of the poly-ubiquitination chain.[1] In the priming step, Vif recruits the RBR-type E3 ubiquitin ligase ARIH2 to carefully mono-ubiquitinate A3G. Based on previous structural studies, Vif binds to RNA and A3G in a manner compatible with the proteins and coenzymes required to mono-ubiquitinate A3G.[2] Based on this observation, as well as its role in promoting A3G binding, it is hypothesized that RNA also plays a role in promoting A3G mono-ubiquitination. The role of RNA was tested in quantitative ubiquitination assays, although no RNA-mediated effect on sA3G ubiquitination was observed (**Fig. 3.2-3.3**). Using the double alanine mutation described above, which should theoretically abolish the interaction between Vif and sA3G, we also observed no adverse effect on sA3G mono-ubiquitination.

This could suggest that RNA only plays a role in Vif-A3G binding; however, it is more likely that Vif and sA3G are bound independently of an RNA-mediated effect. Our molecular glue assay is conducted at ~50 nM concentrations of both sA3G and Vif with 10 molar excess of RNA20. In comparison, the chase reactions are performed at 400 nM Vif, 4,000 nM sA3G, and in the presence or absence of 8,000 nM RNA20. We hypothesize that the differences in an RNA-mediated effect on Vif-A3G binding and A3G mono-ubiquitination could be due to the

differences in concentrations at which these experiments are conducted (**Fig. 4.1**). While useful, fluorescent ubiquitin has a lower limit of detection of 1 μM in pulse-chase assays.

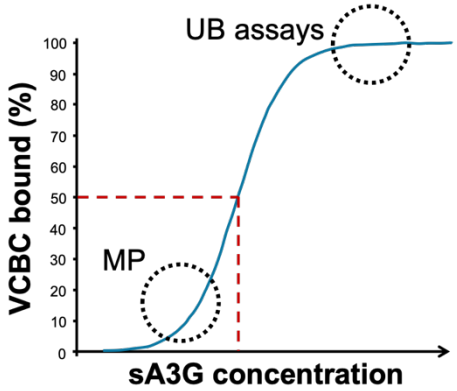

Figure 4.1: **Theoretical binding curve of VCBC bound by sA3G**. The red dotted line represents K_d, while the dotted circles indicate the proposed conditions for binding and ubiquitination experiments.

The actual K_d for sA3G and Vif should be determined using binding assays, such as fluorescence polarization.[3] Similarly, a more sensitive approach could be to use radio-labeled ubiquitin instead of fluorescent ubiquitin during the chase reaction. This could allow visualization of A3G ubiquitination at a concentration closer to the Vif concentration used in the chase reaction. The ubiquitin construct described in this study features a PKA site on the N-terminus, which contains an acceptor serine residue altered to cysteine for fluorescent labeling. Radiolabeled ubiquitin has been previously used to characterize ubiquitination activity and kinetics with other CRL E3 ubiquitin ligases.[4] This assay can also be modified by using other Vif variants and sA3G variants.

These could include optimizing conditions to monitor A3G ubiquitination by precursor lentiviral Vif variants such as SIVrcm Vif. These types of experiments could help address questions related to the molecular arms race between Vif and A3G. Similarly, sA3G with a D128K mutation could be used in combination with Vif mutations at the molecular arms race interface, such as at residue Q83 of HIV-1 Vif. Such experiments could elucidate how viral adaptations manifest on a biochemical level to promote A3G binding and ubiquitination.

Collectively, these could shed light on potential separation-of-function residues in the Vif-RNA-A3G interface.

This pulse reaction can also serve as a framework for expanding the quantitative characterization of A3G ubiquitination. It is interesting to compare the history of knowledge between HIV-1 Vif-mediated A3G ubiquitination and the discovery of CRL E3 ubiquitin ligases. The complex of the prototypical Cullin/RING E3 ubiquitin ligase, SCF, was only discovered in 1997.[5,6] Approximately 5 years later, the first high-resolution structure of the SCF E3 ubiquitin ligase was determined.[7] Around the same time, HIV-1 Vif was discovered to antagonize human A3G, in part, by hijacking a CRL E3 ubiquitin ligase.[8] Since then, kinetic parameters such as K_m and V_{max} have been calculated for ubiquitin transfer reactions catalyzed by various CRL E3 ubiquitin ligases and co-enzymes.

These experiments are not too far from reach, given the HIV-1 Vif-mediated ubiquitination of A3G. In fact, wild-type A3G mono-ubiquitination was previously used to assess the mechanism of ARIH2-mediated ubiquitination activated by a neddylated CRL5-Vif-CBFβ ligase by using various ARIH2 mutations.[9] This ubiquitination assay could be further developed to conduct Michaelis-Menten kinetics on ubiquitin transfer from ARIH2 to A3G bound by the CRL5-Vif-CBFβ ligase. Such experiments could help elucidate how the binding mode of A3G might be impacted by RNA or Vif mutations. Lastly, the ubiquitination assay can be adapted to monitor A3G mono-ubiquitination and poly-ubiquitination simultaneously.[10]

After A3G mono-ubiquitination, ARIH2 dissociates, and the E2 conjugating enzyme CDC34 can then extend the poly-ubiquitin chain. By running an additional pulse reaction to load a different fluorescently labeled ubiquitin onto CDC34, both pulse reactions can be combined with A3G and N8~CRL5-Vif-CBFβ in the chase reaction. Overall, this is an exciting time to study Vif ubiquitination. More careful experiments are needed to fully characterize how residues in the Vif-RNA-A3G interface promote A3G ubiquitination.

REFERENCES

1. Hüttenhain, R. *et al.* ARIH2 Is a Vif-Dependent Regulator of CUL5-Mediated APOBEC3G Degradation in HIV Infection. *Cell Host Microbe* **26**, 86-99.e7 (2019).
2. Li, Y.-L. *et al.* The structural basis for HIV-1 Vif antagonism of human APOBEC3G. *Nature* **615**, 728–733 (2023).
3. Binning, J. M. *et al.* Fab-based inhibitors reveal ubiquitin independent functions for HIV Vif neutralization of APOBEC3 restriction factors. *PLOS Pathog.* **14**, e1006830 (2018).
4. Horn-Ghetko, D. *et al.* Ubiquitin ligation to F-box protein targets by SCF–RBR E3–E3 super-assembly. *Nature* **590**, 671–676 (2021).
5. Feldman, R. M. R., Correll, C. C., Kaplan, K. B. & Deshaies, R. J. A Complex of Cdc4p, Skp1p, and Cdc53p/Cullin Catalyzes Ubiquitination of the Phosphorylated CDK Inhibitor Sic1p. *Cell* **91**, 221–230 (1997).
6. Skowyra, D., Craig, K. L., Tyers, M., Elledge, S. J. & Harper, J. W. F-Box Proteins Are Receptors that Recruit Phosphorylated Substrates to the SCF Ubiquitin-Ligase Complex. *Cell* **91**, 209–219 (1997).
7. Zheng, N. *et al.* Structure of the Cul1–Rbx1–Skp1–F boxSkp2 SCF ubiquitin ligase complex. *Nature* **416**, 703–709 (2002).
8. Yu, X. *et al.* Induction of APOBEC3G Ubiquitination and Degradation by an HIV-1 Vif-Cul5-SCF Complex. *Science* **302**, 1056–1060 (2003).
9. Kostrhon, S. *et al.* CUL5-ARIH2 E3-E3 ubiquitin ligase structure reveals cullin-specific NEDD8 activation. *Nat. Chem. Biol.* **17**, 1075–1083 (2021).
10. Scott, D. C. & Schulman, B. A. Chapter Two - Dual-color pulse-chase ubiquitination assays to simultaneously monitor substrate priming and extension. in *Methods in Enzymology* (ed. Hochstrasser, M.) vol. 618 29–48 (Academic Press, 2019).

Publishing Agreement

It is the policy of the University to encourage open access and broad distribution of all theses, dissertations, and manuscripts. The Graduate Division will facilitate the distribution of UCSF theses, dissertations, and manuscripts to the UCSF Library for open access and distribution. UCSF will make such theses, dissertations, and manuscripts accessible to the public and will take reasonable steps to preserve these works in perpetuity.

I hereby grant the non-exclusive, perpetual right to The Regents of the University of California to reproduce, publicly display, distribute, preserve, and publish copies of my thesis, dissertation, or manuscript in any form or media, now existing or later derived, including access online for teaching, research, and public service purposes.

DocuSigned by:
Leandrew Dailey
63C91E8E5D97450...
Author Signature

12/09/2025 | 3:52 AM
Date